A combined modeling and measurement technique for estimating windblown dust emissions at Owens (dry) Lake, California

Dale Gillette

Fluid Modeling Facility, Applied Modeling Research Branch, Atmospheric Modeling Research Division, Air Resources Laboratory, National Oceanic and Atmospheric Administration, Research Triangle Park, North Carolina, USA

Duane Ono

Great Basin Unified Air Pollution Control District, Bishop, California, USA

Kenneth Richmond

MFG, Incorporated, Lynnwood, Washington, USA

Received 30 January 2003; revised 1 October 2003; accepted 10 November 2003; published 17 January 2004.

[1] The problem of dust emissions from playa sources is an important one both in terms of human health and in terms of global dust issues, distribution of loess, and mineral cycling. A refined method of modeling atmospheric dust concentrations due to wind erosion was developed using real-time saltation flux measurements and ambient dust monitoring data at Owens Lake, California. This modeling method may have practical applications for modeling the atmospheric effects of wind erosion in other areas. Windblown dust from the Owens Lake bed often causes violations of federal air quality standards for particulate matter (PM_{10}) that are the highest levels measured in the United States. The goal of this study was to locate dust source areas on the exposed lake bed, estimate their PM_{10} emissions, and use air pollution modeling techniques to determine which areas caused or contributed to air quality violations. Previous research indicates that the vertical flux of PM_{10} (F_a) is generally proportional to the total horizontal saltation flux (q) for a given soil texture and surface condition. For this study, hourly PM_{10} emissions were estimated using $F_a = K' \times m_{15}$, where m_{15} is the measured sand flux at 15 cm above the surface, and K' was derived empirically by comparing air quality model predictions to monitored PM_{10} concentrations. Hourly sand flux was measured at 135 sites (1 km spacing) on the lake bed, and PM_{10} was monitored at six off-lake sites for a 30 month period. K' was found to change spatially and temporally over the sampling period. These changes appeared to be linked to different soil textures and to seasonal surface changes. K' values compared favorably with other F_a/q values measured at Owens Lake using portable wind tunnel and micrometeorological methods. Hourly trends for the model-predicted PM_{10} concentrations agreed well with monitored PM_{10} concentrations. Dust production was estimated at 7.2×10^4 t of PM_{10} for a 12 month period. A single storm accounted for 9% of the annual dust emissions at 6.5×10^3 t. The modeling results were used to identify 77 km^2 of dust-producing areas on the lake bed that will be controlled to attain the federal air quality standard for PM_{10}. *INDEX TERMS:* 0322 Atmospheric Composition and Structure: Constituent sources and sinks; 0305 Atmospheric Composition and Structure: Aerosols and particles (0345, 4801); 1809 Hydrology: Desertification; 1815 Hydrology: Erosion and sedimentation; *KEYWORDS:* dust, desertification, wind erosion

Citation: Gillette, D., D. Ono, and K. Richmond (2004), A combined modeling and measurement technique for estimating windblown dust emissions at Owens (dry) Lake, California, *J. Geophys. Res.*, *109*, F01003, doi:10.1029/2003JF000025.

1. Introduction

[2] The problem of dust emissions from playa sources is an important one both in terms of human health and in terms of global dust issues, distribution of loess, and mineral cycling. The methodology developed for this study may have practical applications globally to help model the atmospheric effects of wind erosion in other areas. Because of the optical properties of dust and estimations of the large emissions of dust from such sources as the Sahara desert, considerable work has been done on global-scale modeling of dust sources based on first principles of dust emission and large-scale meteorology (for one example of many, see *Ginoux et al.* [2001]). J. Prospero (personal communication, 2002) suggested that dust sources of global importance may

0148-0227/04/2003JF000025

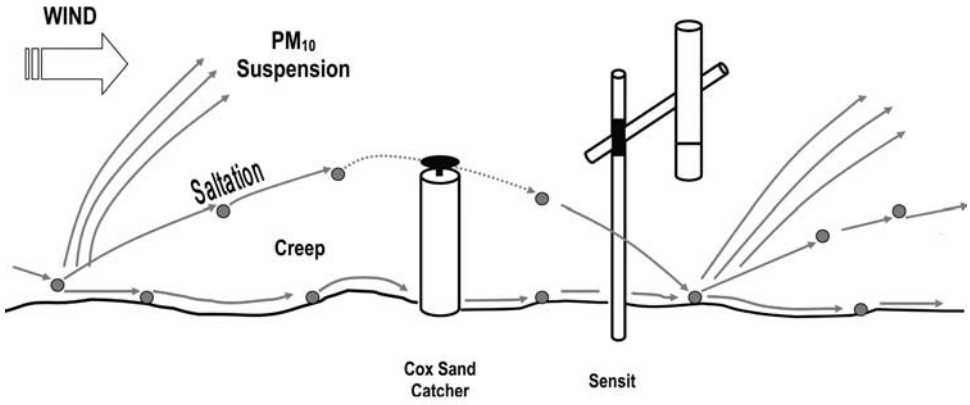

Figure 1. Conceptual depiction of the wind erosion process with a Cox Sand Catcher (CSC) and Sensit positioned in the saltation zone. The mass of saltating particles collected by the CSC was time resolved using the Sensit's electronic response to estimate hourly sand flux at 135 sites. PM_{10} concentrations measured at shoreline PM_{10} monitors were used to infer the ratio of the vertical PM_{10} flux to the horizontal sand flux using dispersion modeling.

be focused on large-scale topographic depressions located in desert regions. Since Owens Lake is a topographic depression of area more than 100 km^2, where the rainfall is less than 15 cm per year, measurements and modeling there could be of value for global-scale models. Future work could include projects such as applying the Owens Lake modeling method to other wind erosion areas, improving global-scale models by validating their predictions against measurements taken at Owens Lake, or improving on first-principle-based emission estimates using the large data set collected at Owens Lake.

[3] The dried bed of Owens Lake in Inyo County, California, is the largest single source of particulate matter pollution in the United States (U.S. Environmental Protection Agency (EPA), *Air Data*, 2003, available at http://www.epa.gov/air/data). The lake bed covers an area approximately 285 km^2 and is a natural saline lake at the terminus of the Owens River. When the Owens River was diverted by the City of Los Angeles into an aqueduct in 1913, it caused the lake to become virtually dry by 1928. A small permanent brine pool is what remains at the lowest part of the basin. It is surrounded by exposed, dry alkali soils. Windblown dust from the exposed lake bed can cause 24 hour average PM_{10} (particulate matter less than a 10 μm nominal aerodynamic diameter) concentrations to exceed 12,000 $\mu g\ m^{-3}$ at the historic shoreline; the federal PM_{10} standard is set at 150 $\mu g\ m^{-3}$. Dust storms often affect the health and welfare of people living within 80 km of the lake. Air pollution levels in communities surrounding Owens Lake exceeded 400 $\mu g\ m^{-3}$ on over 330 days from 1995 to 2002, a level that would trigger a stage 1 health advisory to protect sensitive individuals such as children, the elderly, and people with heart or lung disease [*Great Basin Unified Air Pollution Control District* (*GBUAPCD*), 2003].

[4] In 1993 the U.S. EPA designated the southern Owens Valley as a "serious" nonattainment area for particulate matter. As a result, an air quality plan was developed to implement a control strategy that would bring the area into attainment with federal standards by 31 December 2006. By the end of 2003, about 50 km^2 of the most emissive areas of the lake bed will be controlled by shallow flooding and salt grass cover. The focus of this paper is on the method that was used to locate windblown dust source areas on the Owens Lake bed, to estimate the vertical flux of PM_{10}, and to determine which source areas may cause or contribute to violations of the air quality standards. Through this study, additional areas were identified for control measure implementation that, when controlled, will bring the area into attainment with the PM_{10} standard by the statutory deadline.

2. Method for Estimating the Vertical Flux of PM_{10} Emissions

[5] The working hypothesis for this study was that the vertical flux of PM_{10} (F_a), measured in $g\ m^{-2}\ s^{-1}$, is proportional to the total horizontal flux of sand-sized particles (q); that is,

$$F_a = K \times q, \tag{1}$$

where K is a dimensional constant having units of m^{-1} and q ($g\ m^{-1}\ s^{-1}$) is the horizontal flux of sand-sized particles in a 1-m-thick layer above the ground, as defined in equation (2):

$$q = \int_0^{1m} C(z) V_H(z) dz. \tag{2}$$

Here, $C(z)$ is the concentration of sand-sized grains at height z, and V_H is the horizontal velocity of the sand grains. Experimental evidence for a relationship between F_a and q is discussed in section 2.1.

[6] As shown conceptually in Figure 1, wind erosion involves particles that creep along the ground and sand-sized particles or agglomerates that bounce or saltate across the surface. These creeping and saltating particles loosen other particles and sandblast the surface, causing finer particles, including PM_{10}, to be ejected and to mix vertically in the turbulent air stream. The amount of PM_{10} emitted is generally proportional to the horizontal saltation flux. Using this working hypothesis, F_a could be estimated from sand

flux measurements taken with instruments placed in the saltation zone. This zone typically ranges from the ground to about 1 m above the surface. As discussed in section 3, the ratio F_a/q can be inferred by comparing monitored PM_{10} concentrations with the predicted concentrations from an air quality model. It was assumed that the relationship between F_a and q would remain fairly stable in all but a few exceptional circumstances that may be unique to Owens Lake and that these exceptional circumstances would not account for more than a small fraction of the total PM_{10}. The hypothesis that F_a could be estimated from q made possible a program of efficient sampling based on sand flux measurements that could reveal the location of sources of PM_{10} and also characterize their dust production rates and the time and duration of their activity.

[7] Sand flux is often modeled instead of measured. For example, *Gillette et al.* [1996] and *Owen* [1964] showed that sand flux is generally proportional to $u*$ ($u*^2 - u*_t^2$), where u_t^* is the minimum aerodynamic threshold friction velocity. Previous measurements at Owens Lake showed that despite the uniform appearance of the lake bed, $u_t^*$was highly variable in time and space and would have to be closely monitored if it was used to model q. Because of this variability, we opted not to model q but rather to use a more direct measurement approach. For about the same effort to monitor u_t^* we surmised that one could directly measure q (or a surrogate in this case) and obtain a more accurate sand flux rate.

[8] Although much of the lake bed produces dust, some areas of the 285 km^2 lake bed are consistently covered by a durable crust or are wet and are normally nonemissive. The potentially emissive areas for this study cover about 135 km^2. Figure 2 shows a map of the study area. The portion of the lake bed not covered by the sampling grid generally indicates areas that are normally nonemissive areas. Some source areas inside the grid have been observed to be active all year and may be highly emissive, while others were seasonal and sometimes sporadic. The focus of this study was to better characterize the time, place, and strength of erosion activity for areas within the sampling grid. This information would be used with the Calpuff model [*Scire et al.*, 2000a] to determine in which areas dust controls should be placed. As shown in Figure 2, 135 sand flux sites, spaced 1 km apart, were installed to monitor hourly sand flux rates within the potential erosion area.

[9] The sampling grid was separated into four source areas, as shown in Figure 2, for the purpose of determining large-scale ratios for F_a/q for each area. These areas were selected because of differing geomorphology or source activity that seemed to be somewhat independent of each other. The Keeler Dunes, for example, are sand dunes that differ in geomorphology from the surrounding area and were a frequent source of dust. The ''north area'' and the ''south area'' were seen to be strong source areas that often started at different times during dust storm days. Activity in the ''central area'' was more sporadic than in the other three areas.

2.1. Experimental Evidence for a Relationship Between F_a and q

[10] *Bagnold* [1941] and *Iversen et al.* [1976] showed that there is a minimum aerodynamic threshold friction velocity ($u*_t$) for individual particles to be entrained into the air stream by aerodynamic forces from a smooth surface. This $u*_t$ varies with particle size, roughness of the surface, crusting of the soil surface, soil texture, soil moisture, and salt content [*Gillette et al.*, 1980; *Gillette et al.*, 1982; *Gillette*, 1988; *Breuninger et al.*, 1989]. However, for observations of natural wind erosion for a range of friction velocities smaller than u_t^*, one can find emissions of 10 μm particles [*Cahill et al.*, 1996; *Gillette*, 1977]. Because aerodynamic forces cannot have been responsible for them and because sandblasting of the soil was observed at the time of their emissions, it is highly probable that sandblasting was the dominant mechanism for their input.

[11] The chemical composition of PM_{10} is the same as aggregated coatings of PM_{10}-sized particles on sand-sized particles [*Gillette and Walker*, 1977]. Evidence showed that some individual PM_{10} particles are similar to clay platelets that adhere to the surfaces of larger quartz particles. As the clay particles were not found to exist in the parent soil except as coatings on quartz particles, the airborne particles of the fine mode were almost certainly removed from quartz grains by collisions with the larger particles. The collisions (sandblasting) acted to release portions of aggregated particles and may also have broken the crystalline structure of mineral particles.

[12] Experiments by *Shao et al.* [1993] and *Houser and Nickling* [2001] showed that particle-particle interaction (sandblasting) on an erodible surface is an important and probably dominant mechanism that produces suspended particle flux. Both experiments used wind tunnels, the floors of which contained clay-rich material. Experiments by *Shao et al.* [1993] used finely divided clay, while *Houser and Nickling*'s [2001] experiment used crusted clay material. In both experiments, high winds first yielded exceedingly small amounts of fine material, then large amounts of PM_{10} when sand-sized grains were fed into the stream. Aerodynamic forces alone were able to entrain only small amounts of PM_{10}. At the same wind speeds, however, sandblasting caused steady entrainment of PM_{10}.

[13] *Gillette*'s [1977] work, which simultaneously measured horizontal fluxes of sand-sized particles (q) and vertical PM_{10} fluxes (F_a) on agricultural soils in Texas, formed a body of experimental work with which to compare results at Owens Lake. Gillette's results showed that the ratio F_a/q is consistent when grouped by soil-surface-texture type. Testing the largest group of observations for a single texture type (fine sand) of Gillette's data further led us to accept the null hypothesis that there is no correlation between F_a/q and $u*$ or between F_a/q and q at the 5% level of significance, even though the data showed that q is a strong function of $u*$, in agreement with the theory of *Owen* [1964]. Results by *Nickling and Gillies* [1989] and by *Alfaro and Gomes* [2001] show that F_a/q is largely independent of friction velocity (and also q) for friction velocities well above the threshold friction velocity. However, for friction velocities closer to the threshold friction velocity, F_a/q seems to increase with friction velocity. Since dust emissions close to the threshold friction velocity are much smaller than for those well above, the overall behavior is

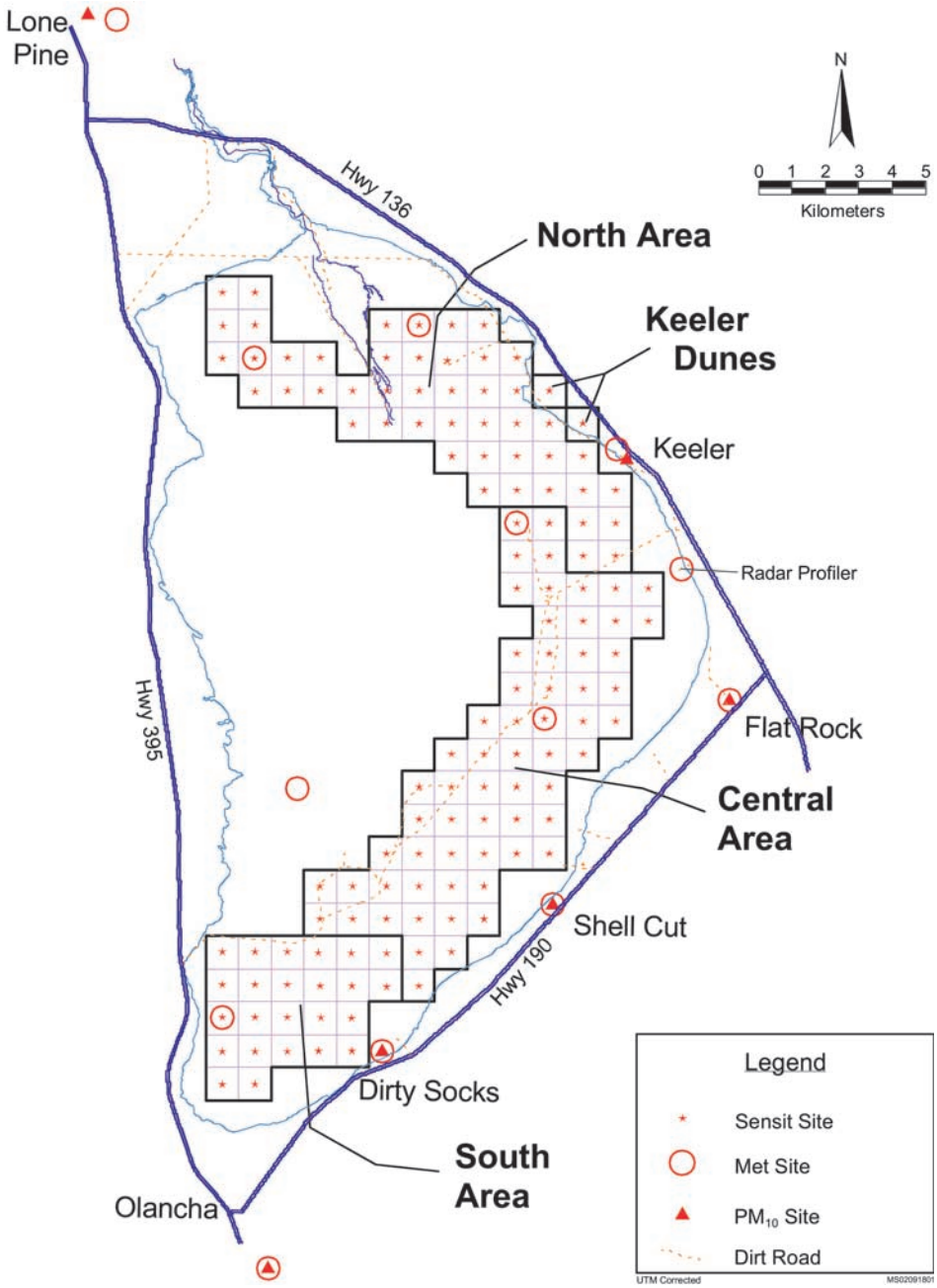

Figure 2. Map of Owens Lake showing the locations of CSCs and Sensit instruments (CSCs and Sensits are at the same locations), PM_{10} monitors, and meteorological (met) towers. Subareas of the dry lake bed are drawn in the north area, south area, central area, and Keeler Dunes.

dominated by F_a/q being largely independent of friction velocity.

2.2. Theoretical Justification for a Relationship Between F_a and q

[14] The sandblasting abrasion rate is proportional to the kinetic energy flux from the sand-sized particles, which is proportional to $u*^3$. *Greeley and Iversen* [1985] summarized a body of research directed toward the aeolian abrasion of rocks and minerals and concluded that the mass of rock or mineral abraded per impact of sand-sized particles is directly proportional to the kinetic energy of the impacting particle. From dimensional analysis, *Gillette and Stockton* [1986] showed that the kinetic energy flux of the wind is proportional to the cube of the friction velocity. Since we can assume that the kinetic energy of the wind is absorbed and carried to the surface by saltating particles at the surface, it follows that the vertical kinetic energy flux carried by saltating particles is proportional to $u*^3$.

[15] According to the classical formulations of *Bagnold* [1941] and *Owen* [1964] as well as to many formulae listed by *Greeley and Iversen* [1985], the horizontal mass flux of saltating sand-sized particles (q) is roughly proportional to $u*^3$ for $u*$ well above threshold. Since both abrasion and the

horizontal mass flux of saltating sand-sized particles are roughly proportional to the same variable, they are therefore roughly proportional to each other. Physically, sand-sized particles localize kinetic energy onto small target areas, while the energy from fluid transfer is spread out over a much larger area.

[16] The *Shao et al.* [1993] expression for the particle flux of suspended particles produced by the impact of saltating particles is

$$F_a = \gamma m_d \frac{g}{\Psi} q f\left(\frac{V_H}{u_*}\right), \tag{3}$$

where Ψ is binding energy, γ is a constant, m_d is mass per particle, g is acceleration of gravity, V_H is the horizontal velocity of the saltating particle, and $u*$ is friction velocity. Both γ and g are constants, and the function $f(V_H/u*)$ has been shown by *Owen* [1964] to be almost constant. Therefore the ratio F_a/q may be expressed as

$$\frac{F_a}{q} = \Gamma \frac{m_d}{\Psi}, \tag{4}$$

where $\Gamma = \gamma g f(V_H/u*)$. Using equation (4) to evaluate F_a/q requires evaluation of the binding energies of suspension-sized particles to the soil and the sizes of typical saltation particles. Such evaluation, however, is a difficult task.

[17] Subtleties within the size distribution of PM_{10} are caused by sandblasting. *Alfaro et al.* [1997] proposed a theory following along the lines of the *Shao et al.* [1993] theory: that the size distributions of the saltating particles are vitally important because the kinetic energy of individual saltating grains, along with the kinetic energy required to release suspendible particles, determines the quantity and size distribution of the suspended aerosol produced by sandblasting. Details of the size distribution of particles smaller than 10 μm are explained in *Alfaro et al.*'s [1997] theory by the sandblasting mechanism.

[18] The theory of *Lu and Shao* [1999] expresses F_a as proportional to either q or to $qu*$. The case in which F_a is proportional to $qu*$ assumes a lifting mechanism other than sandblasting. Such a mechanism should be detectable for Owens Lake by plotting F_a/q versus q, friction velocity, or wind speed. If F_a/q is constant with wind speed, the Owens Lake data will be supportive of a sandblasting mechanism for dust emission. If F_a/q increases roughly proportional to wind speed, the Owens Lake data will be supportive of *Lu and Shao*'s [1999] alternative theory for dust emission.

2.3. Possibility of Non-Saltation-Driven PM_{10} Emissions

[19] Direct suspension of particles may occur when wind speeds are high enough or when sand-sized and larger particles are not the dominant loose particles on a surface. The emission of PM_{10} by the erosion of salt "fluff" has been observed at Owens Lake for brief periods following efflorescence of salt. It is possible that during these brief periods, PM_{10} may be emitted by direct suspension. When only fine-grain sediments are available as loose particles on the surface, direct entrainment can occur without the necessity of sandblasting. Ablation of this fluff does not seem to be correlated with significant sand-sized particle movement at the beginning of dust storms [*Saint-Amand et al.*, 1986]. During the emission of fluff the weak structure of this material may well be crushed by a short initial surge of wind, after which direct aerodynamic entrainment can take place. Also, since the salt fluff is limited in supply, its PM_{10} flux is limited both in total mass and in time. From observations over a period of years we estimate that the contribution of total PM_{10} flux by direct aerodynamic entrainment is small. For example, one of the authors observed dust storms at Owens Lake commencing on 11 March 1993 and ending with rainfall on 25 March 1993. White salt-rich aerosol from fluff was produced for only a half hour to an hour, whereas the total time of wind erosion accompanied by vigorous sand-sized particle movement was about 35 hours.

[20] Finally, the term "sand-sized particles" is used rather than sand in this study because several areas of Owens Lake have little sand but nonetheless have an abundance of sand-sized particles. An example of such an area is the clay rich area to the northeast of Dirty Socks. Here, clay-rich sediments can aggregate and crack into sand-sized aggregates. These sand-sized aggregates act very similarly to sand particles composed entirely of a solid piece of only one mineral.

2.4. *K* Factor Approach and Variability of the Vertical Flux of PM_{10} Dust

[21] K is defined as the ratio of F_a to q:

$$K = F_a/q. \tag{5}$$

For a specific time, K and q are variable quantities for a given location that may be expressed as overall means for the lake bed plus fluctuations for given positions:

$$q = \overline{q} + q' \tag{6}$$

and

$$K = \overline{K} + k'. \tag{7}$$

Both sums of all q' and all k' are zero. For a single storm the vertical flux of PM_{10} dust at a particular square kilometer may be expressed as

$$F_a = \overline{K}q + k'\overline{q} + k'q'. \tag{8}$$

Analysis of *Gillette*'s [1977] data showed that q and K are not correlated; that is,

$$\overline{k'q'} = 0. \tag{9}$$

The middle term on the right-hand side of equation (8) ($k'\overline{q}$) has a mean of zero since the mean of k' is zero. Values of q typically range from zero in some subareas to 1 g cm^{-1} s^{-1} for high wind speeds in a given area of the lake (several km^2 in area); K values typically range two or more orders of magnitude [*Gillette et al.*, 1997a]. Consequently, q has a larger range of variability than K. Our results show that average K factors may change by one order of magnitude and that q may change by three orders of magnitude (excluding $q = 0$).

[22] One can grid the lake surface such that individual horizontal positions west-east and south-north may be labeled "i" and "j," respectively. For successive grid (i and j) positions separated by 1 km an individual measurement of q or F_a at position i, j may be made. Individual measurements of q_{ij} were used to represent q for a square kilometer at position i, j. Then, the rate of total mass of dust produced in a given storm is weighted by the area of each measurement (1 km^2):

$$M_{\text{tot}} = \sum_{ij} K_{ij} q_{ij} (1\,\text{km}^2) = \overline{K} \sum_{i,j} q_{ij} (1\,\text{km}^2) = \overline{K}\overline{q} \sum_{i,j} (1\,\text{km}^2), \tag{10}$$

where

$$\overline{K} = \frac{M_{tot}}{\sum_{i,j} q_{ij} (1\text{km}^2)}$$

and where

$$\overline{q} = \frac{\sum_{i,j} q_{ij} (1\text{km}^2)}{\sum_{i,j} (1\text{km}^2)}.$$

[23] M_{tot} is estimated by measurements of PM_{10} concentrations at the shoreline of the lake bed and modeling of the dust transport from the lake bed. Details of the modeling are available in section 3.6.

[24] The "K factor" method of estimating the vertical flux approximates the vertical mass flux of PM_{10} at each i, j position by using the mean value of K for the area being considered times the individual q_{ij} value at each position for the estimate of $F_{a_{ij}}$. Thus for each position, equation (8) is rewritten as

$$F_{a_{ij}} = \overline{K} q_{ij} + \varepsilon_{ij}, \tag{11}$$

where ε_{ij} is the difference between the true vertical flux of dust at position i, j and $\overline{K} q_{ij}$ (alternatively, the sum of the last two terms of the right-hand side of equation (8)). The mean of ε_{ij} for the entire area is zero. The mean vertical PM_{10} mass flux for the area of the lake considered is

$$\bar{F}_a = \overline{K}\overline{q}. \tag{12}$$

We did not evaluate ε_{ij} of equation (11) since there was no data on k'. This K factor method neglects the error term ε_{ij} to give an approximate value for the individual $F_{a_{ij}}$,

$$F_{a_{ij}} \approx \overline{K} q_{ij}, \tag{13}$$

so that each individual $F_{a_{ij}}$ has an error ε_{ij}. Although individual fluxes at specific locations have associated error with the K factor method, the total flux for the lake is well estimated. The mean K (K factor) is expressed (from equation (10)) as

$$\overline{K} = \sum_{i,j} K_{ij} \left[\frac{q_{ij}}{\sum_{i,j} q_{ij}} \right]. \tag{14}$$

The mean K is often dominated by strong source subregions of the lake that have large sand flux qs. Therefore the mean K (K factor) may not be a good estimator of individual Ks for weak source areas (small qs) if these Ks are significantly different. Consequently, the estimation of K might be representative of primarily the strong source areas of the lake. For example, if the strong sources were eliminated, this method would more accurately represent the weaker source areas. During small emission episodes, K factor measurements are expected to have more variability. This variability may be real, or it may be caused by increased error in the measurement of q since only parts of the square kilometer cells may have active erosion during small events.

[25] *Gillette et al.*'s [1997a] alternative method of measuring vertical PM_{10} fluxes at Owens Lake might improve estimation of F_a at individual points. However, this method would require at least 10 particle concentration measurements for each of our 135 measuring locations on the lake and an accuracy of measurement that may not be technically achievable at this time. We opted to use the K factor method based on the above analysis since it adequately estimated F_a for strong source subareas on the lake surface for the large and highly variable (in time) surface area with which we were concerned.

3. Measurement and Modeling Method for the *K* Factor Approach

[26] To implement the method given in section 2, a combination of measurements and modeling was used. The method relates dust source strength to sandblasting using equation (1) so that F_a could be determined by measuring a grid of q values for the entire lake bed and finding values of K to represent each of the four subareas of the lake bed surface shown in Figure 2. Spatial and temporal Ks were derived empirically by comparing monitored concentrations to concentrations predicted by an air quality model. These spatial and temporal Ks were then used with measured hourly sand flux to estimate F_a and to model ambient PM_{10} concentrations during each dust event.

[27] Hourly sand flux values were determined from a sampling system that used two sand flux instruments. One instrument was a passive sand collector that captured saltating particles, the other an electronic sensor that recorded the hourly particle counts or kinetic energy of the saltating particles. The passive collector was a Cox Sand Catcher (CSC), which collected saltating sand-sized particles. The CSC mass was measured after 1–4 weeks of continuous sampling. The collected mass was then time resolved using electronic readings from a co-located Sensit to estimate hourly sand flux rates during the collection period. Co-located CSCs and Sensits provided hourly sand flux data for 30 months at sites spaced 1 km apart on a 135 km^2 area of the lake bed, as shown on the map in Figure 2. The CSC inlet and the Sensit detector are both positioned in the saltation zone at 15 cm above the surface. This dual measurement technique is shown conceptually in Figure 1.

3.1. Measurement of Long-Term Average *q* Using the Cox Sand Catcher

3.1.1. Efficiency of the Cox Sand Catcher

[28] The K factor approach depends on the measurement of q or a reliable surrogate for q. We chose to measure the

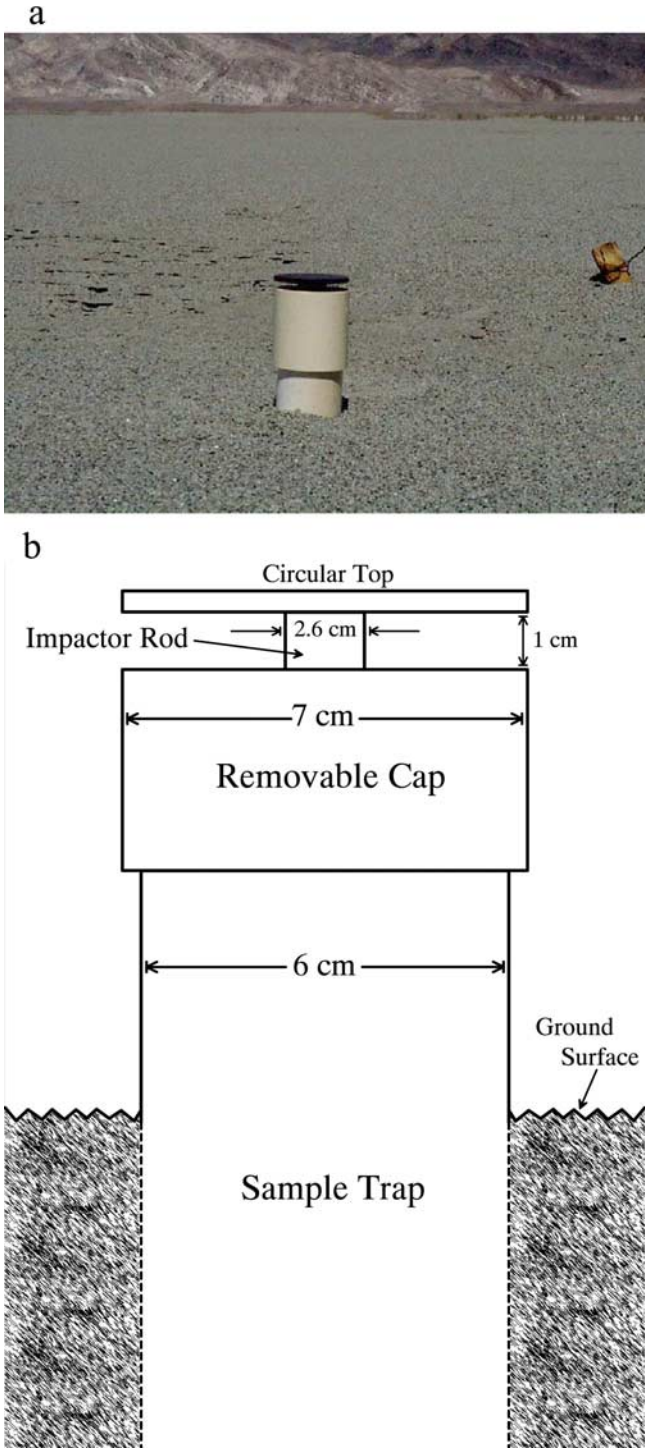

Figure 3. (a) Photograph and (b) schematic drawing of a CSC.

horizontal flux of sand-sized particles at 15 cm as a surrogate for q (see Figure 1). To use this surrogate measurement, we must show that (1) the flux of sand-sized particles at 15 cm can be measured reliably and that (2) the sand-sized particle flux at 15 cm height is linearly related to q. To accomplish the first requirement, the CSC, which was used for this study, was calibrated with a widely used collector, the Big Spring Number Eight (BSNE), manufactured by Custom Products of Big Spring, Texas.

[29] The CSC is a device designed to collect airborne sand-sized particles at 15 cm moving horizontally from all directions. This device has no moving parts, whereas the BSNE is directed into the wind by an attached wind vane. The CSC, which consists of PVC piping, is fabricated by the Great Basin Unified Air Pollution Control District. A schematic drawing of the CSC is given in Figure 3.

[30] BSNE and CSC collectors were placed on the Owens Lake bed surface and were allowed to collect particles during several dust storms during periods of high and low wind speed. Figure 4 shows the mass collected by the BSNE (standard) that points into the wind by an attached vane and the CSC for the same location, collection height, and collection period. The plot shows that the masses captured by the two collectors are linearly related, with an R^2 value of 0.973. It was also determined by comparison with the BSNE that the CSC has an apparent inlet size for flux calculations of 1.435 cm^2. This relationship was used to convert the CSC mass collection into a flux rate by dividing the mass by the apparent inlet size for the time duration of the collection period.

3.1.2. Relation of Mass Flux Measured at 15 cm to q

[31] The second relationship, that of the ratio of a 1 cm^2 sand-sized particle mass flux from 14.5 to 15.5 cm height (m_{15}) to the sand-sized particle mass flux from 0 to 1 m height (q), was also determined empirically. Observed horizontal mass fluxes m (units of mass per length squared per time) at various heights were fitted to *Shao and Raupach*'s [1992] empirical equation for saltation mass flux profiles:

$$m(z) = c \exp\left[az + bz^2\right]. \tag{15}$$

Observed values of $m(z)$ for 10 sets of $m(z)$ profile data obtained continuously on the lake surface were fit to equation (15), and then, the integrated mass flux q, similarly to equation (2), was estimated from

$$q = \int_0^{1m} m dz, \tag{16}$$

where q has the units mass/(length $\times$ time). The mean value of (m_{15}/q), where m_{15} is the mass flux (mass per area per

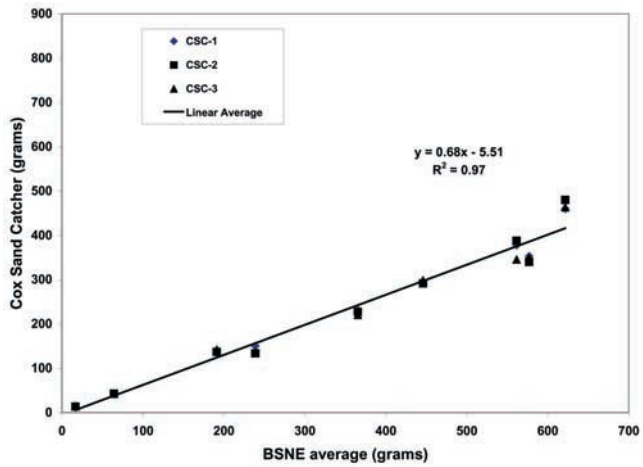

Figure 4. Mass captured by a side-by-side CSC and Big Spring Number Eight airborne particle collector.

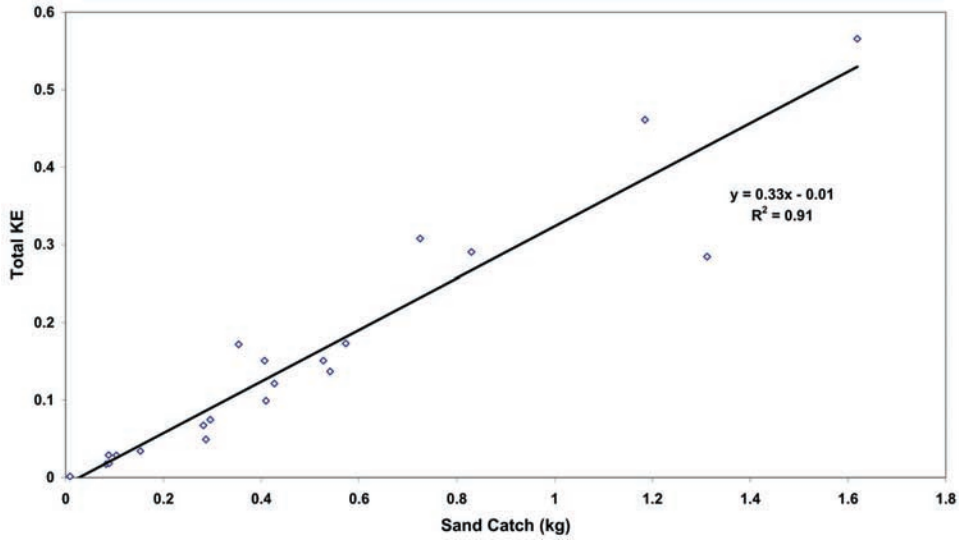

Figure 5. Accumulated airborne mass catch ($\int\int m_{15} dAdt$) at 15 cm height (kg) and Sensit kinetic energy instrumental response integrated over the same sampling period and the same height for side-by-side locations on Owens Lake.

time interval) for heights 14.5–15.5 cm, was 0.024 cm^{-1} (2.4 m^{-1}), with a standard deviation of 0.002 cm^{-1} (0.2 m^{-1}). Values for the shape factors a and b of equation (17) along with their standard deviations in parentheses for the data were 0.078 (0.020) and 0.0004 (0.0003), respectively. The value of the more variable factor c was 2.15 (2.55). *Gillette et al.* [1997b] calculated the ratio of sand-sized particle mass flux from 9.5 to 10.5 cm height to q for many airborne particle profiles at two areas of Owens Lake: near the Dirty Socks Pond and the south area (site of the former Geomet observatory) and at the north area. The value of this ratio was approximately 0.03 cm^{-1}. This value compares favorably to *Gillette et al.*'s [1997b] value, considering that heights at 10 cm would be expected to have larger mass fluxes than at 15 cm. Consequently, this yields the ratio

$$q/m_{15} = 41.7[\text{cm}] = 0.417[\text{m}]. \tag{17}$$

In practice, we used the dimensionless quantity

$$K' = F_a/m_{15} \tag{18}$$

along with the K defined in equation (5). To convert K' to the K of equation (5), equation (18) was used to give

$$K = K' \times 2.4[\text{m}^{-1}]$$

or

$$K = K' \times 0.024[\text{cm}^{-1}]. \tag{19}$$

3.2. Measurement of Hourly Horizontal Mass Fluxes at 15 cm Height

[32] One hour m_{15} values were measured at the centers of a 1-km-spaced square grid work covering the potentially active 135 km^2 of the surface of Owens Lake shown in Figure 2. Hourly mean m_{15} values were calculated by combining information from the sand-sized particle flux values from CSCs (collected over a 10–30 day period) and a collocated Sensit particle flux device. The Sensits and CSCs experienced the same sand-sized particle fluxes at 15 cm height. The Sensit instrument recorded two continuous responses that have been shown to be nearly linearly proportional to mass fluxes [*Gillette et al.*, 1997b; *Stout and Zobeck*, 1996] for carefully controlled conditions, although different mineralogies and size distributions of the particles could lead to different responses for the same mass flux. To estimate hourly sand flux rates, the total mass measurement from the CSC for a sampling period was time resolved using the hourly Sensit readings, which were either based on particle count or kinetic energy readings. For each measured point on the lake surface for the collection period, hourly sand flux was estimated from

$$m_{15} = \Theta S, \tag{20}$$

where S is hourly Sensit response (less its background value) and Θ is the ratio of the CSC total mass collection to the total Sensit response (particle count (PC) or kinetic energy (KE)) for a given collection period. An example of the response of a typical Sensit to the collected CSC mass is shown in Figure 5. Similar plots were generated for each Sensit to check for large deviations in Θ, which may indicate that a Sensit was operating improperly.

[33] The two Sensit continuous responses are called by the manufacturer "KE" and "PC" outputs. The Sensit response for the KE output includes a background which must be subtracted from the KE signal before the integrated Sensit response is converted to m_{15}, as in equation (20). The other output of the Sensit, PC, was also available. This output did not have a background value; however, PC outputs were found to be more limited in range than KE.

[34] A 3 month test of the sand flux network at the start of our program revealed problems with the Sensits that were later resolved to ensure the data quality. Although early tests

showed that the Sensits' particle count or kinetic energy outputs were generally proportional to sand flux as measured by the CSCs, this was not true for all Sensits, and care had to be taken in collecting and interpreting the data. The initial testing also revealed a small number of Sensits with unpredictable outputs, which were revealed by large deviations in Θ when sand catch values were high. These Sensits were quickly identified and removed from the network. Owing to changes in the Sensit construction and design during the period that Sensits were obtained for this study, other anomolies were discovered. The first was the manufacturer's incorporation of different background KE outputs for different batches of Sensits. These individual KE background values were recorded when there was no erosion activity, which was indicated by zero particle counts. The background KE was simply subtracted from the Sensit KE data to correct the data. Some Sensits were found to be too sensitive for high-erosion areas, and the signal would be saturated. These were discovered by analyzing the Sensit to sand catch ratios, Θ, for each sampling period. These Sensits were moved to less active sites. A less apparent problem was discovered during testing of the Sensits with a mechanical tapping device that showed slightly different responses to tapping on different sides of the piezoelectric sensor ring. This may indicate that the piezoelectric ring is not completely uniform. A look at the Sensit data for some sites did show small differences in the Sensit and sand catch relationships for northerly versus southerly dust events. However, because the Sensits are maintained in the same directional orientation and the K factors are only determined when the wind direction is in a line from the Sensit to the PM_{10} monitor, this is unlikely to cause errors in the K factor calculations. In addition, high winds at Owens Lake were observed to be primarily northerly or southerly since they are strongly influenced by the Owens Valley's steep mountain ranges.

3.3. Shoreline PM_{10} Monitoring Data

[35] PM_{10} concentration measurements were taken at six fixed stations at the shoreline locations shown in Figure 2. No stations were placed on the western shoreline that runs north and south because of the rarity of winds strong enough to cause dust emissions with easterly components. Ruprecht and Patashnik Tapered-Element Oscillating Microbalance (TEOM) instruments were placed at the six locations along with meteorological stations. TEOM instruments are used to give hourly PM_{10} concentrations and are operated under standard U.S. EPA protocols. Three monitoring stations are sited in small towns: Keeler, Lone Pine, and Olancha. The other three sites are at locations where the public has access and are frequently impacted by dust plumes: Shell Cut, Flat Rock, and Dirty Socks.

3.4. Surface and Upper-Air Meteorological Data

[36] Figure 2 shows the locations for the 10 m towers. This network of surface stations collects hourly wind data at every location. Surface pressure, temperature, relative humidity, and precipitation are also collected at several of the stations. These data, and, when available, wind data from other field programs, are used as the basis for the construction of a surface wind field. In order to characterize the boundary layer on the lake, there is a 915 MHz radar wind profiler with a radio acoustic sounding system (RASS) being operated at the Dirty Socks station shown in Figure 2. The wind profiler with RASS collects hourly wind and temperature data aloft to investigate vertical wind shear and provide data on the boundary layer structure. The surface and upper-air meteorological data are used with the procedures described in section 3.6 to characterize three-dimensional transport on the lake and provide a link between the source areas and shoreline PM_{10} monitoring program.

3.5. Off-Lake Observations of Source Areas

[37] The locations of PM_{10} source areas on the lake bed are verified by using a total of 13 video cameras at six off-lake view points. Three of the observation points are manned. Hourly mapping of source areas is done during storms at elevated locations in the Sierra Mountains (west of the lake), the Coso Mountains (south of the lake), and the Inyo Mountains (east of the lake). Source area mapping is also augmented after storms by circumscribing erosion areas with GPSs.

3.6. Calpuff Modeling Method Used for Estimation of K Factors

[38] K factors were derived empirically as K' by comparing air quality model predictions using the Calpuff modeling system to observed concentrations at six PM_{10} monitor sites [*Scire et al.*, 2000a]. The three-dimensional wind field for Calpuff was constructed from surface and upper-air observations using the Calmet meteorological preprocessor program. Calmet [*Scire et al.*, 2000b] combines surface observations, upper-air observations, terrain elevations, and land use data into the format required by the dispersion modeling component, Calpuff. Winds are adjusted objectively, using combinations of both surface and upper-air observations according to options specified by the user. In addition to specifying the three-dimensional wind field, Calmet also estimates the boundary layer parameters used to characterize diffusion and deposition by the Calpuff dispersion model.

[39] Calpuff is commonly applied to near-field dispersion where the three-dimensional qualities of the wind field are important. Observations at Owens Lake have frequently shown three-dimensional qualities. The model domain includes a 34 $\times$ 48 km area centered on Owens Lake. The model used a 1 km horizontal mesh, with 10 vertical levels extending from the surface to 4 km aloft. The extent of the model domain was selected to match the 1 km mesh size of the Owens Lake sand-sized particle flux network. A lognormal particle mass versus size distribution was used from Owens lake dust size distribution data [*Niemeyer et al.*, 1999]. The distribution was used to give nine particle size classes, to which deposition velocities were assigned using *Slinn and Slinn* [1980].

[40] K factors were estimated for four areas of the lake bed using the following three steps: (1) generate hourly K' values, (2) screen out K' values that had weak source-receptor relationships, and (3) group K' into different temporal periods for each area of the lake bed. K factors were transformed from the dimensionless K' values by equation (19).

3.6.1. Step 1: Generate Hourly K' Values

[41] Hourly K' values were generated using the Calpuff modeling system [*Scire et al.*, 2000a]. Initially, the emissions at point i, j were estimated to be $F_{a_{ij}} = K'_{\text{init}} m_{15_{ij}}$. K'_{init}

was set arbitrarily to 5×10^{-5} to generate model concentrations that were close to the monitored concentrations. In a postmodeling step, the model results with K'_{init} were compared to monitored concentrations at each of the six PM_{10} monitor sites (TEOM sites). Hourly K' values that would have yielded the same modeled concentrations as those that were monitored were then calculated using equation (21):

$$K' = K'_{\text{init}}[(C_{\text{obs}} - C_{\text{back}})/C_{mod}], \quad (21)$$

where

K'_{init} $= 5 \times 10^{-5}$;
C_{obs} observed hourly PM_{10} concentration ($\mu g\ m^{-3}$);
C_{back} background PM_{10} concentration (assumed to be 20 $\mu g\ m^{-3}$);
C_{mod} model-produced hourly PM_{10} concentration ($\mu g\ m^{-3}$).

3.6.2. Step 2: Screen K' Values

[42] K' was calculated for every hour that had active sand flux in cells which were upwind of a PM_{10} monitor. This excluded hours when the dust source areas were from unmonitored source areas off the lake bed, such as nearby sand dunes. These hourly K' values were then screened to remove hours that did not have strong source-receptor relationships between the active source area and the downwind PM_{10} monitor. For example, the screening criteria excluded hours when the edge of a dust plume may have impacted a PM_{10} monitor site. Because the edge of a dust plume has a very high concentration gradient, a few degrees error in the plume direction could greatly affect $K'>$ as calculated in equation (21). Four individual source areas were chosen, as shown in Figure 2. The data were screened using wind direction information such that at least 65% of the dust concentration recorded by the hourly TEOM measurement at the given location came from the target source area. The screening criteria included the following: (1) modeled and TEOM-measured PM_{10} must both be greater than 150 $\mu g\ m^{-3}$; (2) the wind speed at a 10 m height must be greater than 5 m s^{-1}; and (3) sensit-derived 1 hour m_{15} must be greater than 2 g cm^{-2} h^{-1} in at least one cell that was located within 10 km and ±15° upwind from a PM_{10} monitor site.

3.6.3. Step 3: Group Hourly K' Values Spatially and Temporally

[43] About 1000 hours of screened data were used to generate temporal and spatial K' values: (1) for each storm (event) the average K' is calculated for the four source areas; (2) for each of the four source areas the K' averages are divided into seasonal sets; (3) K' values are calculated for the 50th, 75th, and 90th percentiles for each season for each of the four source areas; (4) model performance is assessed by comparing the model predictions to the monitored TEOM concentrations at each site. This was done using each of the three K' percentiles in step 3 to determine which set provided the best model performance. Equation (19) was later used to convert K' to F_a/q (K factor).

4. Results

4.1. Case Study of a Single Dust Storm, 2–3 May 2001

[44] As an illustration of the Owens Lake dust emission model, a storm that began at 0400 LT on 2 May 2001 and ended at 1200 LT on 3 May 2001 is provided as an example of the method. Figure 6a shows the accumulation of m_{15} mass flux for the duration of a specified time ($\int m_{15} dt = Q_{15}$ (g cm^{-2} per storm)) for the storm duration for each km^2 of the area shown in Figure 2.

[45] Figure 6b shows the superimposition of hourly visual maps of the dust sources (solid lines) and dust plumes (dashed lines) for the 36 hours of the dust storm on the map of Owens Lake. The observations were drawn from elevated (mountain) positions west, east, and south of the lake. These observations do not cover the entire 36 hour storm period (for nighttime hours) so that areas may have measured sand flux (not dependent on visual observations) when no visual observations were possible. The two dominant source areas, the north area and the south area (see Figure 2), show plumes of dust being carried southeast and south, respectively. This divergence of plume directions has been observed previously and has been attributed to the presence of the Coso Mountains, south of the Shell Cut station. Plumes originating in the central source areas were observed for only short distances headed south. Plumes from the western part of the south area were not observed. Plumes from the western part of the north area were observed heading southeasterly across the stable crusted area of Owens Lake. A comparison of Figures 6a and 6b shows that the areas of most intense sand movement coincide with the source areas for the dust plumes, even though areas of less intense sand movement (such as the western parts of the south area) did not coincide with observed plumes. These sand movements possibly occurred during hours when observations were not taken.

[46] Figure 7 shows the 1 hour mean values for wind speed, wind direction, TEOM concentrations, and plume observations at 1300 LT on 2 May 2001. TEOM PM_{10} concentrations increase from a value of 32 $\mu g\ m^{-3}$ upwind of the lake at the Lone Pine station to 2452 $\mu g\ m^{-3}$ directly downwind of the strong south area source. Wind speeds range from 10 to 16 m s^{-1}, and plume directions are consistent with plume directions in the model. The Keeler TEOM registered a much lower concentration than the Dirty Socks TEOM, reflecting the fact that it was not in the direct downwind plume of the north area. The Q_{15} values (horizontal sand-sized particle mass flux measured at a height of 14.5–15.5 cm) for the hour 1300 LT on 2 May 2001 is also shown in Figure 7. All of the source areas shown in Figure 2 are seen to be active during this hour. Sand-sized particle fluxes as high as 118 g cm^{-2} h^{-1} are seen in the north area and as high as 43 g cm^{-2} h^{-1} in the south area. The central area had individual sand-sized particle flux measurements as high as 7 g cm^{-2} h^{-1} near the Shell Cut location.

[47] Figure 8 shows cumulative vertical fluxes of PM_{10} ($\int F_a dt$) for the full duration of the 2–3 May 2001 dust storm for each cell of the map. K factors used for Figure 8 were produced by completing steps 1 and 2 in sections 3.6.1–3.6.2. Of the four source areas shown in Figure 1, the north area and the south area are seen to be strong source areas on 2–3 May. The central area was seen to be only partially active: west of the Flat Rock station and north and west of the Shell Cut station. The Keeler Dunes area was a strong, although small, dust source area.

[48] The K' component of the PM_{10} emission, proportional to the K factor (see equation (19)), was calculated by

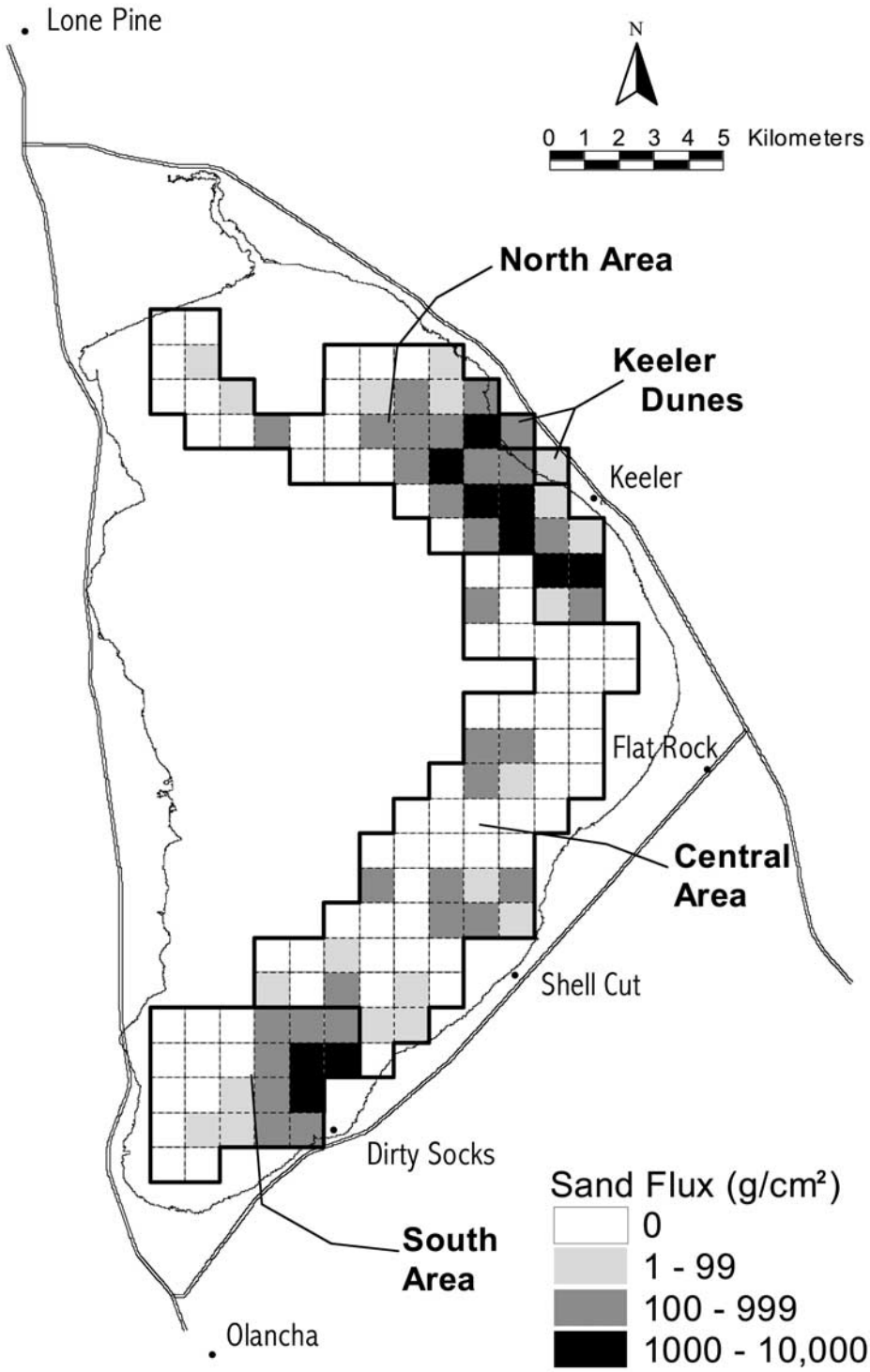

Figure 6a. Accumulated sand-sized particle flux ($\int m_{15} dt$) at 15 cm height for a dust storm at Owens Lake, California, on 2–3 May 2001. Shading in each 1 km^2 grid cell shows the range of accumulated sand-sized particle flux at 15 cm height (g cm^{-2}) for that cell for the entire storm.

the methods given in sections 3.6.1–3.6.3. *K* factors were calculated for each hour and for each source area by completing steps 1 and 2 of sections 3.6.1–3.6.2. A plot of hourly *K* factors is shown in Figure 9a for the south area, the north area, and the central area. The differences for source areas of the three TEOM locations are reflected in the lower values of the north area compared to those from the south and central areas during the early part of the storm. Central area *K* factors are often larger than south area *K* factors. A feature common to all three source areas is that they possess larger *K* factor values at the start of the storm compared to the later values. *Saint-Amand et al.* [1986]

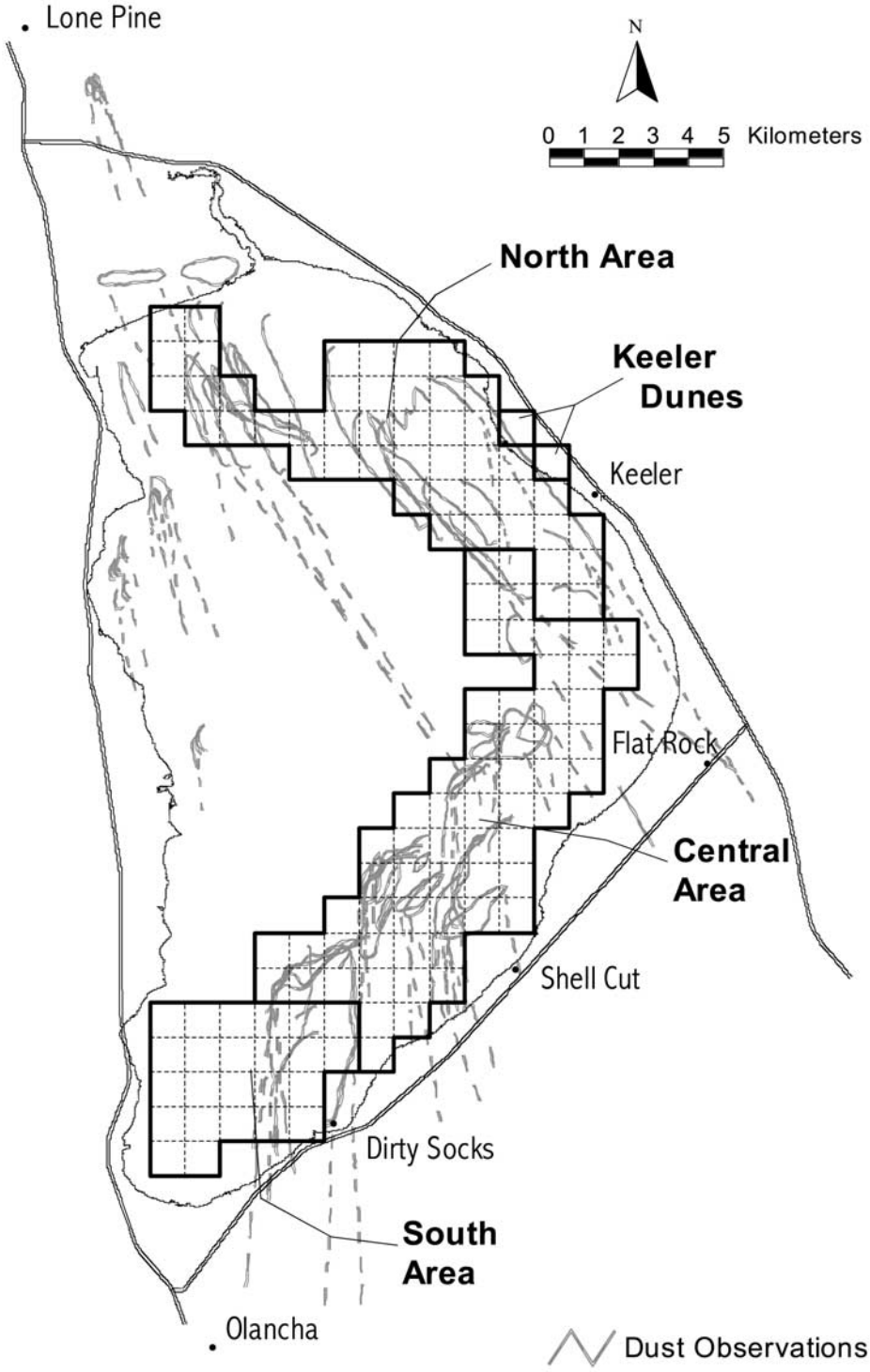

Figure 6b. Dust plume boundaries for a dust storm at Owens Lake, California, on 2–3 May 2001. Observed hourly boundaries of dust plumes are superimposed on the map of Owens Lake.

suggested that softer crustal material at Owens Lake reflects differing mineralogical crystallization that is separated at a 15°C boundary; harder crusts are formed at temperatures greater than 15°C (late spring and summer), while softer crusts are formed at cooler than 15°C (winter and early spring). This might explain the initial rapid lowering of the *K* factors as removal of more easily abraded material (softer crust), exposing a harder crust below. After the decrease of the *K* factors of the first day of the storm, the *K* factors of the second day were rather consistent in time.

[49] Figure 9b compares observed versus predicted hourly PM_{10} concentrations ($\mu g\ m^{-3}$) at the Dirty Socks TEOM for the 2–3 May 2001 episode at Owens Lake using the average *K* factors for the north, central, and south areas for the dust

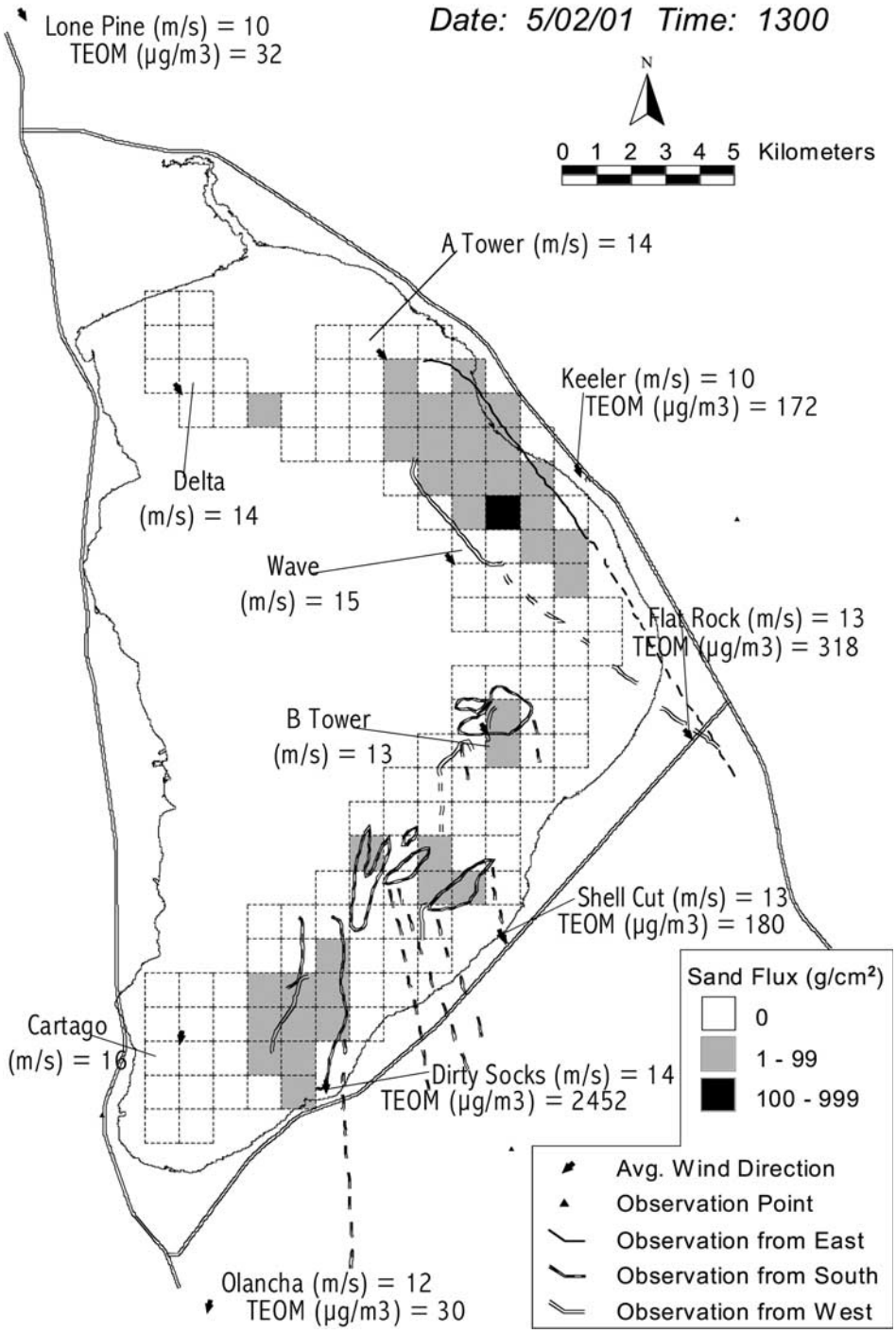

Figure 7. Map of Owens Lake, California, during a dust storm on 2–3 May 2001 at 1300 LT. The range of 1 hour time-integrated sand-sized particle flux at 15 cm height (g cm^{-2}) is shown in each 1 km^2 grid cell by shading. The boundaries of dust plumes are superimposed.

storm and the average K factor for the previous storm for the Keeler Dunes. The storm average K factors for each source area were used to calculate individual vertical fluxes of dust using the m_{15} at every location for each hour of the storm. These F_a values were used in the transport model to calculate concentrations at the location of the Dirty Socks TEOM. Although changes in the hourly concentration trends were predicted, the comparisons show that the hourly concentration at Dirty Socks was underpredicted for concentrations >10,000 µg m^{-3} and <100 µg m^{-3} for this event. Underestimation of strong emissions and overestimating weak emissions was expected by using the storm mean K factors.

4.2. Summaries of Q_{15} for 1 July 2000–30 June 2001

[50] Figure 10 shows Q_{15} for each square kilometer of the Owens Lake grid for 1 year: 1 July 2000–30 June 2001.

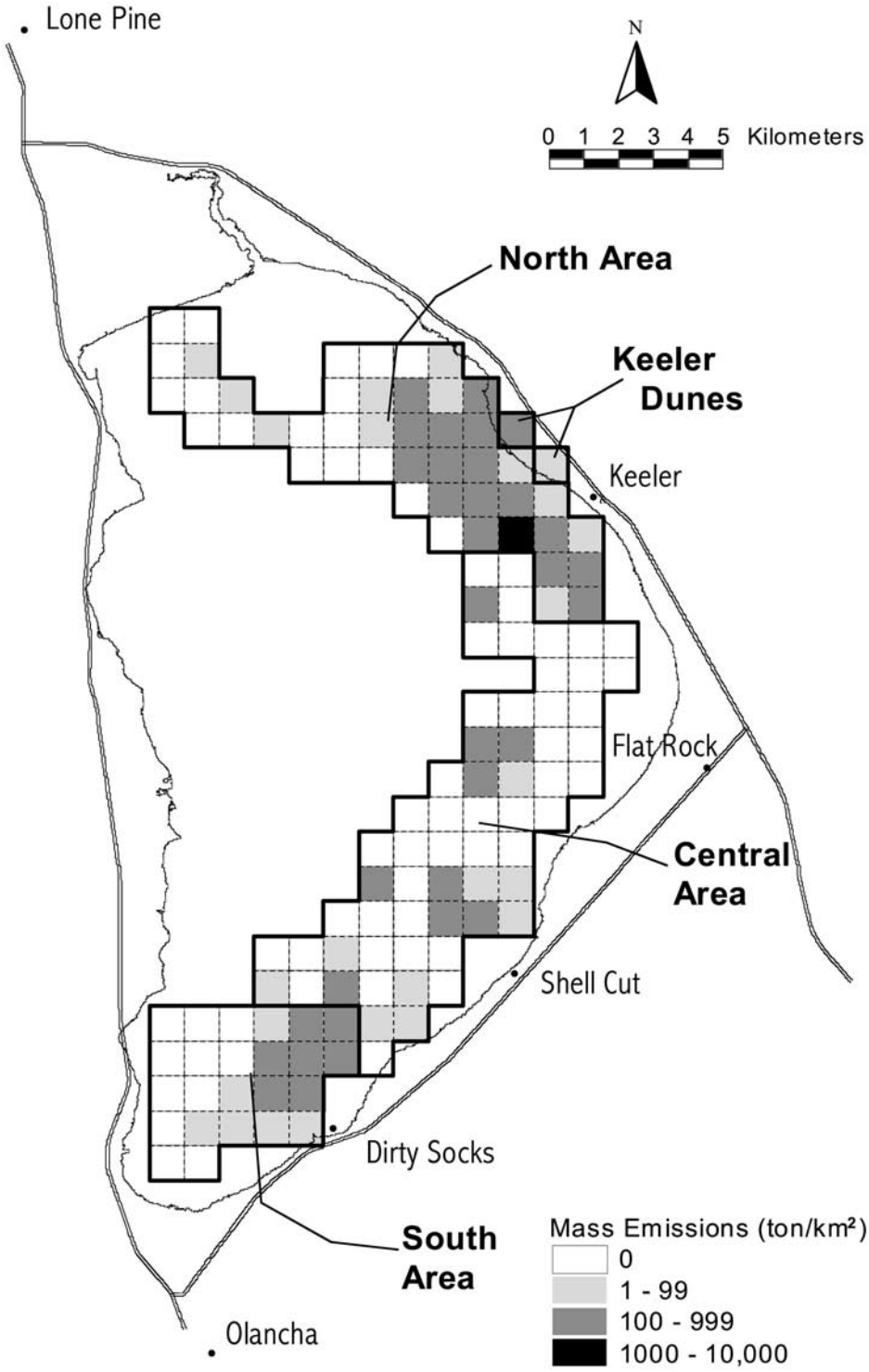

Figure 8. The range of time-integrated PM_{10} particle flux ($\int F_a dt$) (t km^{-2}) for a dust storm for each 1 km^2 grid cell on 2–3 May 2001 at Owens Lake, California, versus location on Owens Lake, shown by shading. The boundaries of four distinct dust emission source areas are shown.

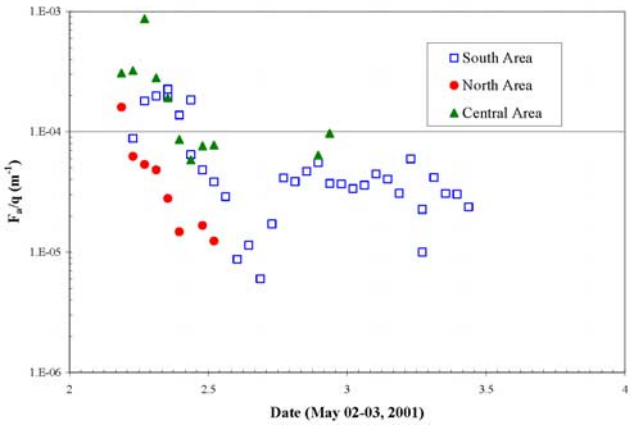

Figure 9a. Hourly K factors (estimated F_a/q (m^{-1})) for the 2–3 May 2001 dust storm developed for three source areas on Owens Lake (south area, north area, and central area).

Since zero Q_{15} values represent areas that have not had sand motion in a significant quantity, the pattern of nonzero Q_{15} is roughly equivalent to the pattern of dust-emitting surface for this time period. The pattern of Q_{15} provides a rough picture of the strongest dust source areas of the Owens Lake bed.

4.3. Variation of the *K* Factor for Two Source Areas During One Storm

4.3.1. Hourly *K* Factors Developed for the South Area

[51] Figure 11 shows hourly K factors (F_a/q estimated using equation (19)) developed from using steps 1 and 2 of sections 3.6.1–3.6.2. The K factors are plotted versus four independent variables: day, PM_{10} mass concentration measured by the TEOM, wind speed, and maximum Sensit flux during the 1 hour sampling period. The time period is January 2000–June 2002. Figure 11a, showing hourly K factors versus day, suggests that the highest K factors occur in the spring of the year, although there is also large scatter for all the times. The observation of large K factors in the spring is consistent with the discussion of the storm of 2–3 May 2001 in section 4.1. Figure 11c shows a considerable scatter of F_a/q versus wind speed. The K factors show a slight reduction of scatter for higher wind speed along with an absence of small K factors for the strongest winds. Likewise, the maximum Sensit flux during the hour of sampling shows reduction of scatter for the highest maximum Sensit response. Finally, there seems to be a small trend of the K factor with PM_{10} (TEOM) concentration. We feel that the high-PM_{10} concentrations occur only during times of effective dust production (high F_a/q values) so that Figure 11b shows that the dust concentration correlates with efficiency of dust production.

4.3.2. Hourly *K* Factors Developed From the North Area

[52] Figure 12 shows the hourly K factors developed for the north area by using steps 1 and 2 of sections 3.6.1–3.6.2. Figures 12a–12d show the same general features as Figures 13a–13d did for the south area, although with fewer data points. They also suggest a possible slight correlation of K factor with wind speed and maximum Sensit flux. Figure 12c possibly suggests a higher correlation than does Figure 11c. The north and south areas both have sandy soil textures, which may help explain the similarity in K factor ranges and values in Figures 11 and 12.

4.4. Summary of the Temporal and Spatial F_a/q Values for Owens Lake

[53] Table 1 summarizes the temporal and spatial F_a/q values that were generated from the screened K' data. The 75th percentile storm average values are summarized because they were found to provide the best model performance on high PM_{10} days (see the complete method for calculating K factors in sections 3.6.1–3.6.3). For other purposes, such as for individual storms, day-specific storm average values may be more accurate. All four areas showed temporal trends in K factors. These differences might be attributed to the different soil textures that were found in a soil survey of the surface soil textures. Average K factor values were more stable over different areas of Owens Lake than were sand flux rates, which typically varied by three orders of magnitude for sites in the same area. The clay-dominated central area had the highest average K factors but was normally less than a factor of ten different from the lowest K factor during any period. The Keeler Dunes, north area, and south area, which all had sandy soil textures, normally had less than a factor of three difference between the areas.

4.5. Total PM_{10} Mass Fluxes for the Period 1 July 2000–30 June 2001

[54] To calculate cumulative vertical mass flux $\int F_a dt$ for an extended period of time, we used K factors that were equal to the 75th percentile of the hourly K factors for each of the source areas; that is, for each source area and each season we multiplied the 75th percentile K factor for each season times hourly m_{15} fluxes to calculate PM_{10} vertical fluxes (F_a). Comparisons of observed concentrations with concentrations developed from using the seasonal 50th, 75th, and 90th percentile K factors showed that the 75th percentile K factors gave the best agreement between calculated and observed concentrations.

[55] The estimated cumulative vertical mass flux for all locations shown in Figure 2 at Owens Lake is shown in

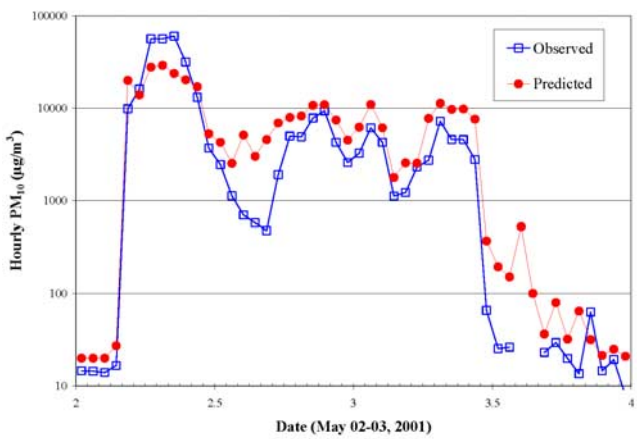

Figure 9b. Observed versus model-calculated hourly PM_{10} concentrations ($\mu g\ m^{-3}$) at the Dirty Socks TEOM for the 2–3 May 2001 episode at Owens Lake.

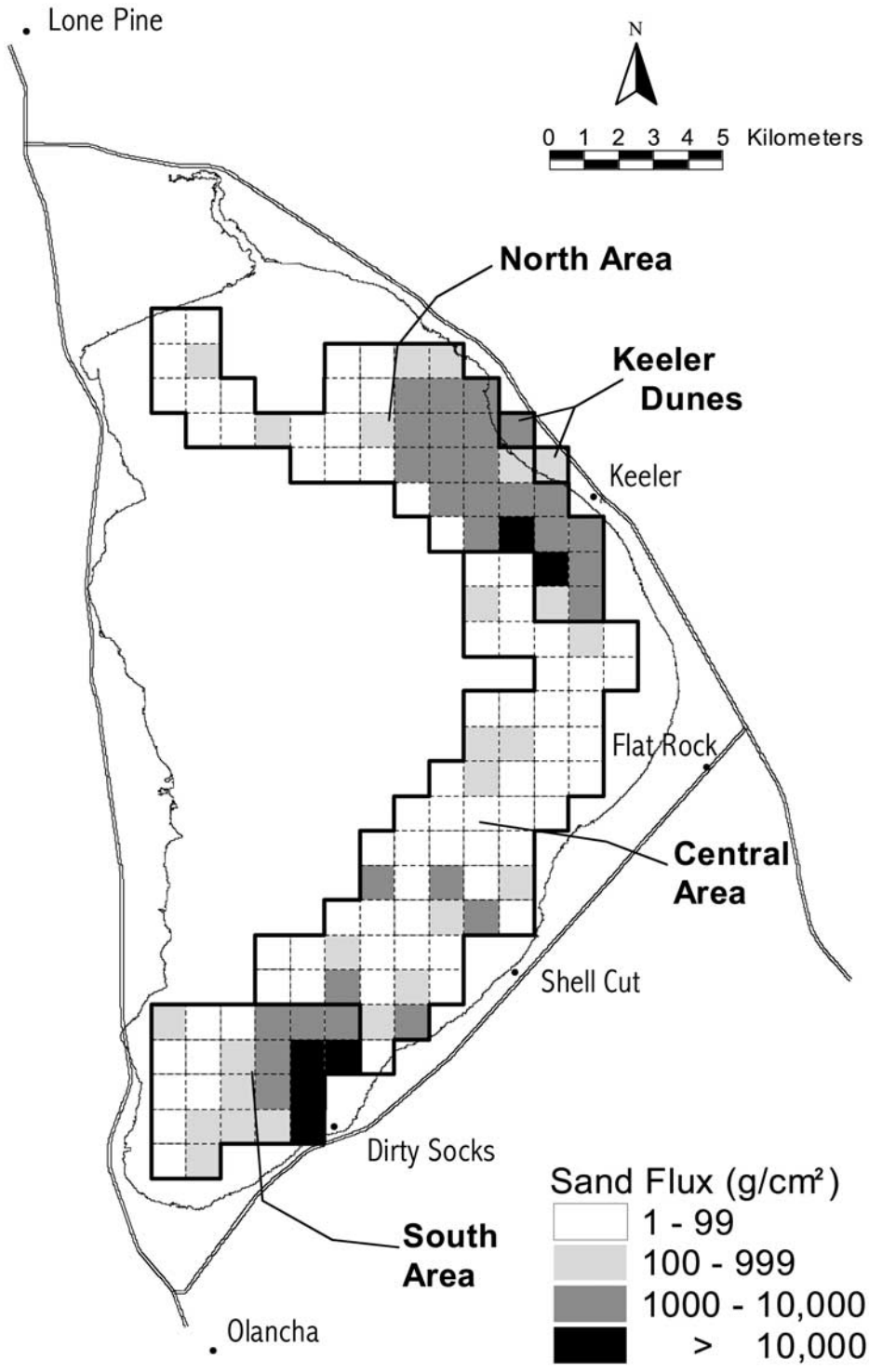

Figure 10. The range of time-integrated sand-sized particle flux at 15 cm height ($\int m_{15} dt$) (g cm^{-2}) for all dust storms at Owens Lake, California, from 1 July 2000 to 30 June 2001 versus location on Owens Lake, shown by shading. The boundaries of four distinct dust emission source areas are shown.

Figure 13 for the 1 year period from 1 July 2000 to 30 June 2001. This 1 year time period was chosen since 1 July 2000 was the first time the entire Owens Lake surface was fully instrumented, while after 1 July 2001, dust controls were placed on the lake bed, which significantly reduced dust production. Figure 13 shows a pattern of PM_{10} integrated vertical fluxes for the 1 year period that shows some similarities in patterns of the time integrated Q_{15}s for the 2 day storm of 2–3 May 2001 shown in Figure 6a. The storm of 2–3 May 2001 was the largest dust-producing event for the 1 year period. The similar patterns for PM_{10} integrated vertical flux of the largest single storm and that

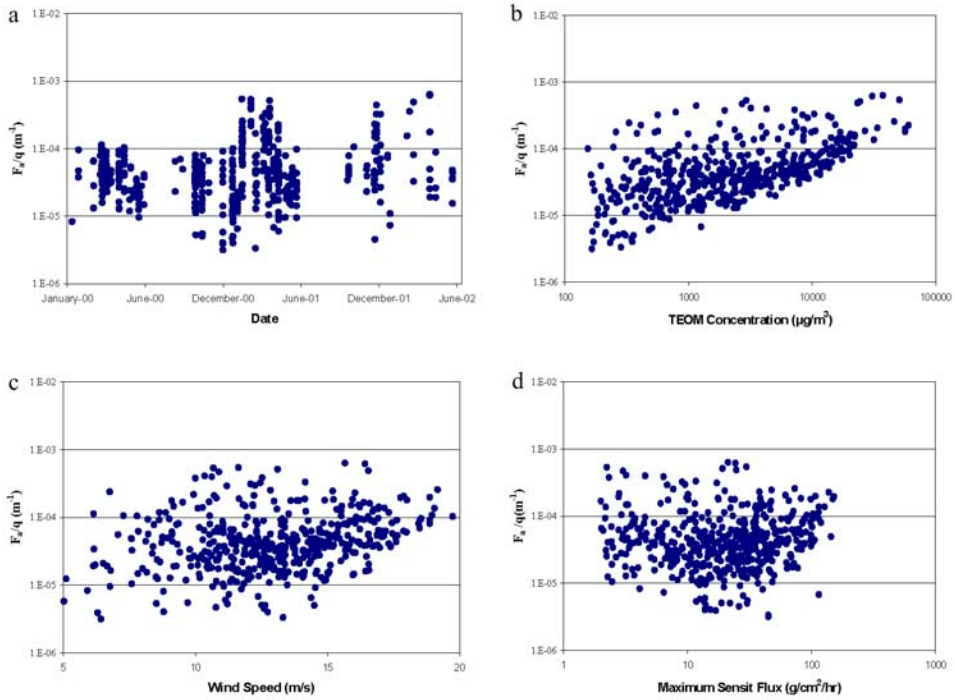

Figure 11. Hourly K factors (F_a/q (m^{-1})) developed for the south area of Owens Lake for January 2000–June 2002 versus (a) day, (b) hourly mean PM_{10} mass concentration obtained by TEOM, (c) wind speed (m s^{-1}), and (d) maximum Sensit flux (maximum m_{15}). Data are restricted to the conditions given in section 2.2.6.

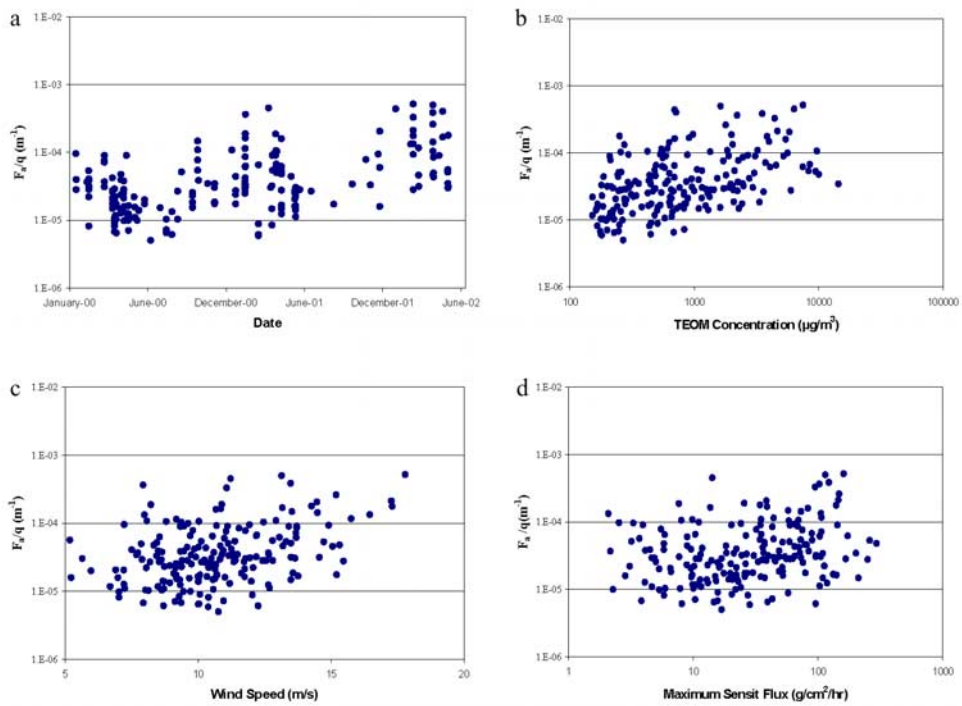

Figure 12. Same as Figure 11, but for the north area.

Table 1. Temporal and Spatial 75th Percentile Storm Average F_a/q Values at Owens Lake[a]

Period					
Start	End	Keeler Dunes	North Area	Central Area	South Area
1 Jan. 2000	3 Feb. 2001	1.2×10^{-4}	0.5×10^{-4}	1.6×10^{-4}	0.5×10^{-4}
4 Feb. 2001	18 April 2001	1.2×10^{-4}	0.5×10^{-4}	6.2×10^{-4}	1.6×10^{-4}
19 April 2001	30 Nov. 2001	1.2×10^{-4}	0.5×10^{-4}	1.5×10^{-4}	0.5×10^{-4}
1 Dec. 2001	8 March 2002	4.7×10^{-4}	4.9×10^{-4}	8.6×10^{-4}	1.0×10^{-4}
9 March 2002	18 April 2002	1.4×10^{-4}	1.3×10^{-4}	1.9×10^{-4}	2.1×10^{-4}
19 April 2002	30 June 2002	1.4×10^{-4}	1.3×10^{-4}	1.6×10^{-4}	0.4×10^{-4}

[a]Values are in m^{-1}.

for the yearly accumulated total suggest that the south area is usually the largest dust-producing part of the lake surface. For the year of measurements, our examination of individual storm events showed that the north area occasionally is the largest dust contributor of the four areas, that the Keeler Dunes are a small but constant contributor of dust, and that the central area produces less dust than the north area or south area. Figure 14 shows the frequency distribution of daily total PM_{10} integrated vertical flux for the entire lake for the same year. The distribution shows that ~50% of the dust storms emit <10 t in a 24 hour period. Dust storms were observed to be highly sporadic through the year, although the largest total emissions usually take place in the months of March–May, and the smallest total emissions take place in the months of June–August. For the 1 year period the total PM_{10} emission from the surface of Owens Lake was 7.2×10^4 t. The storm of 2–3 May 2001 accounted for 6.5×10^3 t, or 9%, of the yearly emissions.

5. Discussion

5.1. Consistency of *K* Factors With Other Work

[56] Here, we compare F_a/q ratios as determined using the K factor method with F_a/q ratios obtained from small-scale portable wind tunnel and micrometeorological methods. When comparing the source area average or lake-wide average K factor with individual K values obtained for small areas on the lake, it is important to remember that K factors may be regarded as weighted means of individual Ks (see equation (14)); that is, the K factor is a weighted sum of the individual K_{ij}s: Where there is relatively small q_{ij}, there is not much influence by the local K_{ij} on the K factor, and a properly measured small-scale K_{ij} might (but does not necessarily) differ from a properly measured large-scale average K factor. Therefore a requirement for comparison of our mean K factors with the mean of wind tunnel Ks was that the wind tunnel test area not lie in an area of below-average sand flux.

[57] K factors vary inversely as the binding energy of the surface sediment according to equation (4). At Owens Lake, binding energy (corresponding to surface cohesion crusting or lack thereof) depends on the soil type, salt content, moisture content at the surface, and temperature conditions during surface dehydration [*Saint-Amand et al.*, 1986]. These conditions are often unpredictable and vary on both large and small scale and in time, making the binding energy a very elusive parameter.

[58] *Alfaro and Gomes*'s [2001] theoretical work on the effect of binding energies and kinetic energies of saltating sand particles shows that variability resulting from differing sizes of sand grains, differing velocities of sand grains, and binding energies can result in a small-scale variation of K more than a factor of 10. Such variability is seen in the K results for similar soils of *Gillette et al.* [1997a].

[59] The K factor method from this study averages over a large dust-emitting area contributing to one dust plume and over a 1 h time period. Small-scale K factors can also be determined using wind tunnel methods on the lake bed or micrometeorological methods. For example, we compare in section 5.1.2 the averages of many wind tunnel Ks measured in one of the four source areas of Owens Lake with the time-averaged K factors for the period of measurement. We also compare a small-scale K value obtained in 1993 with K factors for the south area. Although this comparison was less desirable than one having data collected at the same time, it takes advantage of historical data.

5.1.1. Measurements of F_a/q Ratios in the South Area, March 1993

[60] Micrometeorological measurements of the vertical fluxes of PM_{10} and sand-sized particle fluxes on the south area of Owens Lake taken 11 March 1993 by *Gillette et al.* [1997a] gave a ratio of PM_{10} flux to sand-sized particle mass flux (F_a/q) of 2.8×10^{-4} m^{-1}. The K factors for the south area (representative of the area in which the *Gillette et al.* [1997a] measurements were obtained) are roughly consistent in the springtimes of 2001 and 2002, shown in Figure 11. This range of K factors is consistent with the F_a/q ratios found by *Gillette* [1977] for sand-textured soils and suggests that the binding energy and size of saltating particles for the tested surface material at the south area of Owens Lake is of the same order as that for sandier soils. Vertical fluxes of PM_{10} aerosol for 11 March 1993, estimated by Sun photometry for a large section of Owens Lake, were reported by *Niemeyer et al.* [1999]. These values were used to calculate values of F_a/q by using q values reported by *Gillette et al.* [1997a] for the same storm in the south area of the lake bed. After removing one anomalous value (~2×10^{-2} m^{-1}), explained by *Niemeyer et al.* [1999] as being due to the pooling of dust by the Sierras, the range of their values (~1×10^{-4} m^{-1}–1×10^{-3} m^{-1}) enclosed the *Gillette et al.* [1997a]F_a/q value.

5.1.2. Wind Tunnel *K* Factors Versus *K* Factors of This Study

[61] *Nickling and Brown* [2002] used a portable wind tunnel to measure small-scale F_a/q. In their measurements the surface of Owens Lake was used as the floor of the wind tunnel, which was carefully lifted onto the surface, avoiding disturbance. Two kinds of F_a/q measurements were made:

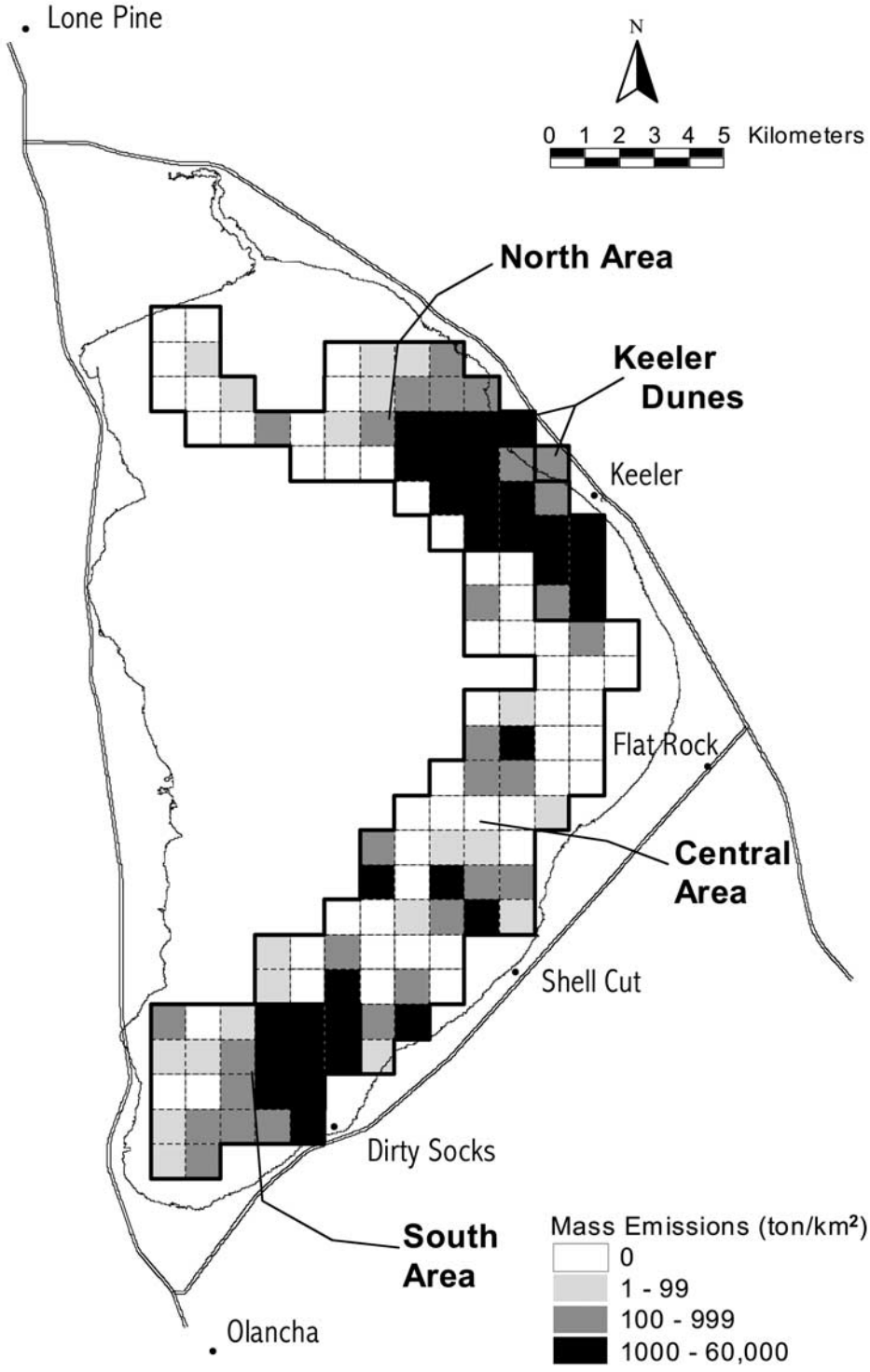

Figure 13. The range of accumulated PM_{10} particle flux ($\int F_a dt$) (t km^{-2}) for all dust storms at Owens Lake, California, from 1 July 2000 to 30 June 2001 versus location on Owens Lake, shown by shading. The boundaries of four distinct dust emission source areas are shown.

with or without clean sand being fed into the upwind part of the tunnel. Since the total floor area of the wind tunnel was 12 m^2, the tunnel measurements represent very local F_a/q values. In contrast, our K factors represent mean F_a/q values for areas of about 3×10^7 m^2.

[62] Comparison of our K factors with the wind tunnel F_a/q are given in Table 2 [*Nickling and Brown*, 2002]. Our values and the wind tunnel values for the same lake areas are within a factor of three. Considering the large differences in averaging area and the standard deviations of the

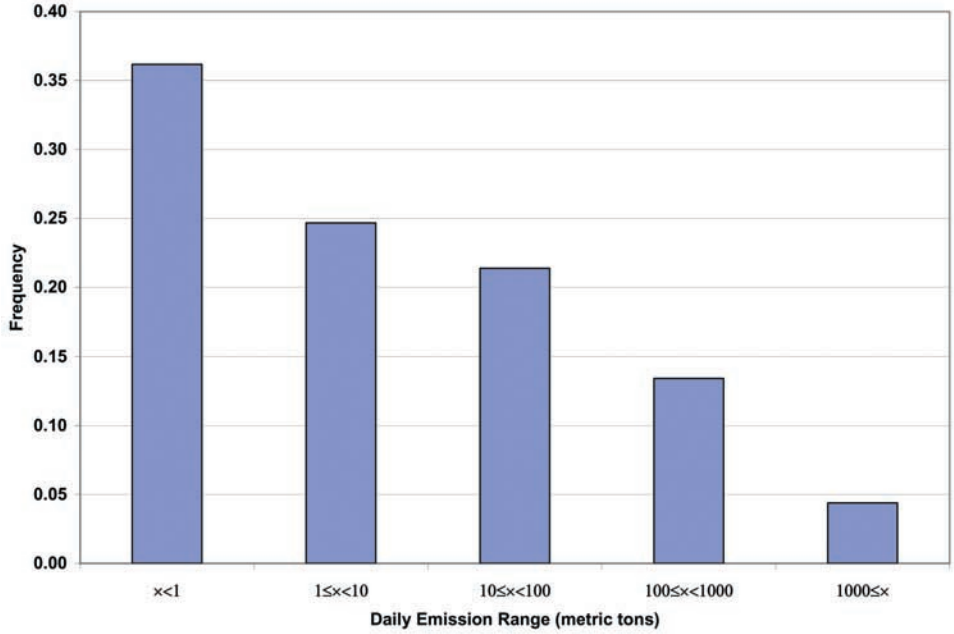

Figure 14. Frequency of daily total mass of PM_{10} emissions from the entire Owens Lake surface ($\int F_a dA$) (t d^{-1}) versus the daily emission range for the period 1 July 2000–30 June 2001. Data are restricted to the conditions given in section 3.6.

means, we consider the comparisons to be within the range of natural variability of F_a/q found on the lake bed.

5.2. Implication of *K* Factor Data on the Dust Emission Mechanism

[63] Our *K* factor data from Owens Lake may constrain the nature of PM_{10} emissions. Figure 11 shows that for the south area, our *K* factors seem to be approximately constant versus maximum sand-sized particle flux for wind speeds less than ~17 m s^{-1}. For these wind speeds we favor the impact kinetic energy mechanism. However, the appearance that *K* factors increase for wind speeds >17 m s^{-1} may indicate that the *Lu and Shao* [1999] excavation mechanism might increase PM_{10} emissions at very high wind speeds.

5.3. Dispersion Model Uncertainty

[64] The Calpuff modeling system and meteorological data collected at Owens Lake have been used to characterize transport and examine the relationships between the shoreline PM_{10} observations and on-lake Sensit data in order to infer PM_{10} emission rates. The variability found in the derived emission fluxes and *K* factors are influenced by both actual physical effects and the uncertainties associated with the modeling system. Uncertainties in the modeling system could be caused by the following.

[65] 1. The first cause could be the inaccurate specification of diffusion and transport caused by errors in model formulation or the lack of sufficient horizontal and vertical meteorological data. Diffusion estimates from the model have been checked qualitatively by comparing plume depths and widths mapped by off-lake observers with model predictions. Observed plume widths appear to be well described by the model, but in some instances, calculated plume trajectories differ from those mapped by the off-lake observers. For some of the high-wind events, plume depths seem to be underpredicted by the model; the video cameras suggest more turbulent vertical diffusion. For such events the derived vertical PM_{10} emission fluxes may be underestimated in this analysis.

[66] 2. A second cause could be the insufficient resolution of the Sensit array. The 1 km spacing of the Sensit array is insufficient to capture some of the smaller source areas during the less severe dust events. For the larger dust events on the lake the source areas are much larger than 1 km^2, and

Table 2. Comparison of Our Mean *K* Factors With Small-Scale Mean *K* Factors Determined by a Wind Tunnel Without Feed

Time Period			Average *K* Factors	
Start	End	Area	Our *K* Factor (Large-Scale F_a/q), m^{-1}	Wind Tunnel (Small-Scale F_a/q), m^{-1}
1 Jan. 2000	3 Feb. 2001	north	4.3×10^{-5}	5.5×10^{-5}
1 Jan. 2000	3 Feb. 2001	Keeler Dunes	8.4×10^{-5}	3.1×10^{-5}
4 Feb. 2001	18 April 2001	central	57.8×10^{-5}	23.3×10^{-5}
4 Feb. 2001	18 April 2001	south	14.2×10^{-5}	15.8×10^{-5}
19 April 2001	30 Nov. 2001	central	13.7×10^{-5}	38.4×10^{-5}
19 April 2001	30 Nov. 2001	south	4.8×10^{-5}	7.4×10^{-5}

the horizontal spacing of the Sensits appear to be adequate to characterize sand motion.

[67] 3. A third cause could be the insufficient coverage of the Sensit array. A number of off-lake source areas have been observed to affect the shoreline PM_{10} monitoring network. With the exception of the Keeler Dunes northwest of Keeler, sand fluxes in these sources areas are not recorded by either CSCs or Sensits and are not included in the model simulations. To the extent possible, wind direction data have been used to filter out the contribution of off-lake sources during the analysis. During periods of highly variable winds or when circulation is more complex, use of the hourly average wind direction at the PM_{10} monitoring site may not always be effective in removing the influence of sources not simulated in the analysis.

[68] 4. It is possible that for low $u*$ the wind stress varies strongly with atmospheric stability regimes [see, e.g., *Chu et al.*, 1996]. However, for dust emission episodes, $u*$ was large enough to preclude large errors. Averaging times for $u*$ were 1 hour.

[69] For the most part, the uncertainties mentioned above are unbiased and result in scatter in the derived K factors and inferred emission fluxes. Large-scale spatial and seasonal differences in the derived variables, when based on ensemble statistical measures, are expected to be more robust.

5.4. Variability for F_a/q Observed at Low Wind Speeds

[70] Figures 11 and 12 show that the variability of F_a/q is higher for low wind speeds and smaller for larger wind speeds. In our case the large variability in F_a/q for low wind speeds may be caused by the patchiness of threshold velocities and minimum energies for fine particle production by sandblasting. Patchiness of threshold friction velocity causes large variability of q near the threshold velocity, and variability of minimum energy for emission of PM_{10} particles causes large variability for sand kinetic energies near the threshold. The variability of threshold velocity is caused by differing sizes of sand particles, variable roughness, and crusting of the soil. The variability of minimum energy for PM_{10} emission by sandblasting (i.e., particle-particle bonding) may be affected by variable crusting of the soil. As wind speed increases, threshold velocity is exceeded for a wide variety of particles, and roughness is smoothed by sandblasting. Evidence of smoothing of the Owens Lake surface during the storm of 11 March 1993 [*Gillette et al.*, 1997a] was observed when rough, crusted soil was sandblasted and developed into smooth, loose sand. Consequently, for higher wind speeds the F_a/q ratio would be expected to have less variablility with wind speed.

5.5. Application of the K Factor Method to Control Dust Sources at Owens Lake

[71] A practical application of the work described above, and the primary intent of this study, was to identify the dust source areas that can cause or contribute to violations of the NAAQS for PM_{10}. By incorporating the dust emissions into the Calpuff model as described in section 3.6, we calculated the contribution from each square kilometer source area on the lake bed to shoreline PM_{10} concentrations at over 400 locations (virtual receptors.) These source contributions were estimated for every hour during the 30 month study period. Because K' only changed seasonally (Table 1), emission trends were primarily driven by hourly sand flux rates, which varied by three orders of magnitude during dust events. As a result of the model predictions, it was determined that $\sim$77 km^2 of the lake bed will require dust control measures to reduce emissions to the point that compliance with the NAAQS can be expected. The dust control area generally corresponds to the shaded cells in Figure 13, with the exclusion of a few cells that had low dust emissions and did not significantly impact shoreline areas.

[72] The air quality plan, based on this model prediction, anticipates the application of shallow flooding, managed vegetation, or gravel on the identified dust source areas. These control measures are expected to reduce dust emissions by 99%. Implementation of control measures on the identified source areas are anticipated to be completed by 31 December 2006, in accordance with the federal Clean Air Act [*GBUAPCD*, 2003].

5.6. Application of the K Factor Method to Other Large-Scale Dust Sources

[73] Following J. Prospero's (personal communication, 2002) observation that large-scale topographic depressions located in desert regions may be dust sources of global importance, Owens Lake may provide a good case study since it is a topographic depression of more than 100 km^2 in area where rainfall is <15 cm yr^{-1}, and it is a prolific source of dust. The measurement and modeling technique used at Owens Lake to estimate detailed patterns of dust emissions may help to improve large-scale modeling in other topographic depressions and important dust-producing areas. Our technique was based on the present inability to model the saltation flux on the surface of Owens Lake because of changes in crusting, the addition of loose sand to the surface by wind transport from upwind, and changes in the mineralogy hydration state caused by temperature changes, resulting in soft crusts during the winter months and hard crusts during the summer months. Consequently, we chose to measure saltation flux rather than predict it. On the other hand, our results (Figures 11 and 12) show that K factors change seasonally (probably largely because of the above mineralogical change) and with location on the surface (probably because of sediment texture differences). However, K factors are more well behaved and more predictable than are saltation fluxes. It would seem that for topographic depressions, our technique of measurement of q and measurement and modeling of K factors would be applicable. In applying this technique, care must be taken to design sufficient measurements to detect changes in K factors by season and location on the source area, as we found for Owens Lake. These changes are caused by the presence in the dust source sediments of hydrating minerals that change state in the annual temperature range expected and the presence of differing size distributions and compositions of sediments in the source area.

[74] At a larger scale, one may find the measurement part of our strategy to be quite expensive; that is, measurement of q on a 1 km scale for a depression significantly larger than Owens Lake would require more instrumentation. We found that the scale of 1 km reproduced observed dust plumes to the degree necessary for the purposes of predicting sites causing significant air pollution. However, it is possible that one could also model large-scale depressions

using a coarser sampling network and less time resolved saltation flux sampling points for depression sediments that are more homogeneous than those at Owens Lake.

[75] In the case where saltation fluxes can be modeled accurately the extensive measurements of saltation flux required in our method could be replaced by modeled saltation fluxes. In the authors' opinion, modeling saltation flux is very difficult to do well. It depends strongly on the ability to predict the threshold velocity, which may be highly variable due to nonuniform surface conditions, such as variations in the soils and seasonal effects on the surface crust. However, saltation flux modeling for places with uniformly eroding surfaces could be done reasonably well for a single event since a constant threshold velocity could be used. In the case where saltation flux modeling is used instead of measurements, K factors could be determined by modeling combined with measurements of dust concentrations around the depression perimeter. In cases where such measurements are not possible, rough estimates may be possible by using representative K factors. For example, for a large-scale depression, values of K might resemble those from Owens Lake or K measured in other areas if general characteristics of the sediment are similar. For cases where measurements of q and K are not available, wisely chosen K values and well-modeled q values could be used to estimate F_a.

[76] If global climate models project changes in the frequency distribution and mean of winds, the frequency of wind storms will likely change. A detailed analysis of the change of dust storm strength and frequency would require the wind speed frequency distribution and the distribution of threshold velocities for wind erosion of the surface. The amount of increase/decrease was modeled by *Gillette* [1999] using a simplified probability distribution for wind speed and threshold velocity. When threshold velocities remain constant and velocities of surface winds increase, the probabilities for wind erosion events increase. If threshold velocities decrease and velocities of surface winds increase, one would expect a much larger increase.

6. Conclusions

[78] Windblown dust from the Owens Lake bed often causes violations of federal air quality standards for particulate matter (PM_{10}) that are the highest levels measured in the United States. A refined method of modeling atmospheric dust concentrations due to wind erosion was developed for Owens Lake that combines real-time saltation flux measurements with ambient dust-monitoring data. A combination measurement and modeling method was shown to be a useful estimator for the vertical flux of PM_{10} from a large wind-eroding area. The measured quantities were (1) hourly m_{15} (sand-sized particle mass flux at 15 cm height), from which q mass fluxes were calculated using equation (17), and (2) hourly PM_{10} concentrations on the shore of Owens Lake at six different locations. The modeled quantity was the K factor, a variable that expresses the ratio of the vertical flux of PM_{10} (F_a) to the horizontal flux of sand-sized particles (q). The product of the K factor and q is the vertical flux of PM_{10} mass. The quantity q is, in turn, related to m_{15}, the horizontal flux of sediment flux at a height of 15 cm. This combination method is quite useful since m_{15} was shown to be a smooth function in space but highly sporadic in time. By measuring m_{15} on a grid network with 1 km separation over 135 km^2, we were able to estimate hourly q rates for the entire lake bed. The measured variability of m_{15} over time and space would have been difficult to predict due to strong dependence on soil crusting and changes in soil aggregation that are not well modeled at this time. Temporal trends in K factors appeared to correspond to seasonal changes in the surface soil conditions. The K factors developed for Owens Lake agreed favorably with K factors for which both horizontal mass flux and vertical PM_{10} flux were measured in the southern part of Owens Lake in 1993. In addition, wind tunnel measurements of K factors obtained at locations found to be the most prolific producers of dust on the lake were also found to be in reasonable agreement with the K factors developed for the four subregions of the lake, for roughly the same year and season.

[79] By multiplying measured sand flux rates with the model-derived K factors, it was possible to estimate the vertical flux of PM_{10} for Owens Lake. For the 1 year period 1 July 2000–30 June 2001 the total PM_{10} emission from the surface of Owens Lake was 7.2×10^4 t. The largest single storm (on 2–3 May 2001) accounted for 9% of those emissions. Dust emissions were found to vary with season. The largest emissions took place in the months of March–May, while the smallest emissions take place in the months of June–August. As a result of this study, dust source areas on 77 km^2 of the lake bed were identified and were determined through dispersion modeling to have caused or contributed to federal air quality violations. Dust control measures to bring the area into attainment with air quality standards are expected to be implemented on these source areas by 31 December 2006.

[80] **Acknowledgments.** The authors gratefully acknowledge the guidance and encouragement of Ellen Hardebeck, Air Pollution Control Officer of the Great Basin Unified Air Pollution Control District. Scott Weaver, Michael Slates, and Jim Parker were extremely helpful in working with the data. Bill Cox led the field work and designed the Cox Sand Catcher. Nik Barbieri, Chad Stein, Guy Davis, and Dan Johnson accomplished the demands of keeping the experiment going on the bed of Owens Lake. Mention of trade names or commercial products does not constitute endorsement or recommendation for use. Funding for this study was provided by the City of Los Angeles Department of Water & Power to the Great Basin Unified Air Pollution Control District under a regulatory mandate to control windblown dust at Owens Lake (California Health and Safety Code §42316).

References

Alfaro, S. C., and L. Gomes (2001), Modeling mineral aerosol production by wind erosion: Emission intensities and aerosol size distributions in source areas, *J. Geophys. Res.*, *106*, 18,075–18,084.

Alfaro, S. C., A. Gaudichet, L. Gomes, and M. Maillé (1997), Modeling the size distribution of a soil aerosol produced by sandblasting, *J. Geophys. Res.*, *102*, 11,239–11,249.

Bagnold, R. (1941), *The Physics of Blown Sand and Desert Dunes*, 265 pp., Methuen, New York.

Breuninger, R., D. Gillette, and R. Kihl (1989), Formation of wind erodible aggregates for salty soils and soils with less than 50% sand composition in natural terrestrial environments, in *Paleoclimatology and Paleometeorology: Modern and Past Patterns of Global Atmospheric Transport*, edited by M. Leinen and M. Sarnthein, pp. 31–63, Kluwer Acad., Norwell, Mass.

Cahill, T., T. Gill, J. Reid, E. Gearhart, and D. Gillette (1996), Saltating particles, playa crusts and dust aerosols at Owens (dry) Lake, California, *Earth Surf. Processes Landforms*, *21*, 621–639.

Chu, C. R., M. B. Parlange, G. G. Katul, and J. D. Albertson (1996), Probability density functions of turbulent velocity and temperature in the atmospheric surface layer, *Water Resour. Res.*, *32*, 1681–1688.

Gillette, D. A. (1977), Fine particulate emissions due to wind erosion, *Trans. Am. Soc. Agric. Eng.*, *29*, 890–897.

Gillette, D. A. (1988), Threshold friction velocities for dust production for agricultural soils, *J. Geophys. Res.*, *93*, 12,645–12,662.

Gillette, D. A. (1999), A qualitative geophysical explanation for "hot spot" dust emitting source regions, *Contrib. Atmos. Phys.*, *72*, 67–77.

Gillette, D. A., and P. H. Stockton (1986), Mass, momentum, and kinetic energy fluxes of saltating particles, in *Aeolian Geomorphology*, edited by W. G. Nickling, pp. 35–56, Allen and Unwin, Concord, Mass.

Gillette, D. A., and T. R. Walker (1977), Characteristics of airborne particles produced by wind erosion of sandy soil, High Plains of west Texas, *Soil Sci.*, *123*, 97–110.

Gillette, D. A., J. Adams, A. Endo, D. Smith, and R. Kihl (1980), Threshold velocities for input of soil particles into the air by desert soils, *J. Geophys. Res.*, *85*, 5621–5630.

Gillette, D. A., J. Adams, D. Muhs, and R. Kihl (1982), Threshold friction velocities and rupture moduli for crusted desert soils for the input of soil particles into the air, *J. Geophys. Res.*, *87*, 9003–9015.

Gillette, D. A., G. Herbert, P. H. Stockton, and P. R. Owens (1996), Causes of the fetch effect in wind ersoion, *Earth Surf. Processes Landforms*, *21*, 641–659.

Gillette, D. A., D. W. Fryrear, T. E. Gill, T. Ley, T. A. Cahill, and E. A. Gearhart (1997a), Relation of vertical flux of particles smaller than 10 μm to total aeolian horizontal mass flux at Owens Lake, *J. Geophys. Res.*, *102*, 26,009–26,015.

Gillette, D. A., D. W. Fryrear, J. B. Xiao, P. Stockton, D. Ono, P. J. Helm, T. E. Gill, and T. Ley (1997b), Large-scale variability of wind erosion mass flux rates at Owens Lake: 1. Vertical profiles of horizontal mass fluxes of wind-eroded particles with diameter greater than 50 μm, *J. Geophys. Res.*, *102*, 25,977–25,988.

Ginoux, P., M. Chin, I. Tegen, J. M. Prospero, B. Holben, O. Dubovik, and S.-J. Lin (2001), Sources and distributions of dust aerosols simulated with the GOCART model, *J. Geophys. Res.*, *106*, 20,255–20,273.

Great Basin Unified Air Pollution Control District (GBUAPCD) (2003), Owens Valley PM10 planning area demonstration of attainment site implementation plan 2003 revision, *Board Order 031113-01*, Bishop, Calif.

Greeley, R., and J. Iversen (1985), *Wind as a Geological Process on Earth, Mars, Venus and Titan*, 333 pp., Cambridge Univ. Press, New York.

Houser, C. A., and W. G. Nickling (2001), The emission and vertical flux of PM_{10} from a disturbed clay-crusted surface, *Sedimentology*, *48*, 255–268.

Iversen, J. D., J. B. Pollack, R. Greeley, and B. R. White (1976), Saltation threshold on Mars: The effect of interparticle force, surface roughness, and low atmospheric density, *Icarus*, *29*, 381–393.

Lu, H., and Y. Shao (1999), A new model for dust emission by saltation bombardment, *J. Geophys. Res.*, *104*, 16,827–16,842.

Nickling, W., and L. Brown (2002), PM_{10} dust emissions at Owens Lake California, *Contract UOG 00-1*, 75 pp., Great Basin Unified Air Pollut. Control Dist., Bishop, Calif.

Nickling, W., and J. Gillies (1989), Emission of fine grained particulates from desert soils, in *Paleoclimatology and Paleometeorology: Modern and Past Patterns of Global Atmospheric Transport*, edited by M. Leinen and M. Sarnthein, pp. 133–165, Kluwer Acad., Norwell, Mass.

Niemeyer, T. C., D. Gillette, J. DeLuisi, Y. Kim, W. Niemeyer, T. Ley, and T. Gill (1999), Optical depth, size distribution and flux of dust from Owens Lake, California, *Earth Surf. Processes Landforms*, *24*, 463–479.

Owen, P. R. (1964), Saltation of uniform sand grains in air, *J. Fluid Mech.*, *20*, 225–242.

Saint-Amand, P., L. Matthews, C. Gaines, and R. Reinking (1986), Dust storms from Owens and Mono Lakes, *Tech. Publ. 6731*, Nav. Weapons Cent., China Lake, Calif.

Scire, J. S., D. G. Strimaitis, and R. J. Yamartino (2000a), A user's guide for the Calpuff dispersion model (version 5), Earth Tech, Concord, Mass., Jan.

Scire, J. S., D. G. Strimaitis, and R. J. Yamartino (2000b), A users's guide for the Calmet meteorological model (version 5), Earth Tech, Concord, Mass., Jan.

Shao, Y., and M. R. Raupach (1992), The overshoot and equilibrium of saltation, *J. Geophys. Res.*, *97*, 20,559–20,564.

Shao, Y., M. R. Raupach, and P. A. Findlater (1993), Effect of saltation bombardment on the entrainment of dust by wind, *J. Geophys. Res.*, *98*, 12,719–12,726.

Slinn, G., and S. Slinn (1980), Predictions for particle deposition on natural waters, *Atmos. Environ.*, *14*, 1013–1016.

Stout, J. E., and T. M. Zobeck (1996), Establishing the threshold conditions for soil movement in wind eroding fields, in *Proceedings of the International Conference on Air Pollution From Agricultural Operations*, pp. 65–71, Midwest Plan Serv., Iowa State Univ., Ames.

D. Gillette, Fluid Modeling Facility, Applied Modeling Research Branch, Atmospheric Modeling Research Division, Air Resources Laboratory, National Oceanic and Atmospheric Administration, MD-81, Research Triangle Park, NC 27711, USA. (gillette.dale@epa.gov)

D. Ono, Great Basin Unified Air Pollution Control District, 157 Short Street, Bishop, CA 93514, USA. (duaneono@yahoo.com)

K. Richmond, MFG, Incorporated, 19203 36th Avenue West, Suite 101, Lynnwood, WA 98036, USA. (ken.richmond@mfgenv.com)